5. SITE 509[1]

Shipboard Scientific Party[2]

HOLES 509, 509A

Date occupied: November 27, 1979

Date departed: November 27, 1979

Time on hole: 7 hr., 7 min.

Position (latitude; longitude): 0°35.34′N; 86°07.89′W

Water depth (sea level; corrected m, echo-sounding): 2676.8

Water depth (rig floor; corrected m, echo-sounding): 2686.8

Bottom felt (m, drill pipe): 2704.4

Penetration (m): 32.3

Number of cores: 9

Total length of cored section (m): 32.3

Total core recovered (m): 32.61

Core recovery (%): 100

Oldest sediment cored:
Depth sub-bottom (m): 32.3
Nature: Foraminifer nannofossil ooze
Age: 270–440 × 10^3 y.
Measured velocity (km/s): MnO: 2.22; Granular green clay: 1.72; Pelagic sediment: 1.51

Basement:
Depth sub-bottom (m): 32.3
Nature: Basalt

Principal results: Two holes were cored (509 and 509B) and three heat-flow measurements taken at Site 509, which is located in the same area as IPOD Leg 54, Site 424. The sediment of the off-mound Hole 509 contains no hydrothermal material. This observation demonstrates that contrary to the conclusion made on Leg 54, the hydrothermal material has no regional extension at this site, and, therefore, the sub-bottom reflectors observed by Lonsdale (1977) must have some other origin. Hole 509 contains siliceous remains down to the bottom of the sedimentary column; whereas in the sediment sections from other off-mound holes, the lower halves are almost devoid of siliceous microfossils.

The overall thickness and lithologic sequence of the mound sediment column is similar to Sites 506 and 507. Hydrothermal sediments are found on the mounds site only. The fossil assemblages are essentially identical to those of Sites 506 and 507. Pore-water chemistry and heat-flow data suggest rapid flushing by upward convection.

Magnetic properties measurements on the sediments are very similar to Sites 506 and 507. Heat-flow measurements and pore-water sampling were conducted in Hole 509A.

HOLES 509B, 509C, 509D

Date occupied: November 28, 1979

Date departed: November 28, 1979

Time on hole: 6 hr., 17 min.

Position (latitude; longitude): 0°35.33′N; 86°07.93′W (Hole 509B). 0°35.33′N; 86°07.89′W (Hole 509C). 0°35.37′N; 86°07.89′W (Hole 509D)

Water depth (sea level; corrected m, echo-sounding): 2686.8

Water depth (rig floor; corrected m, echo-sounding): 2696.8

Bottom felt (m, drill pipe): 2701.8

Penetration (m): 33.8

Number of cores: 8

Total length of cored section (m): 33.8

Total core recovered (m): 32.63

Core recovery (%): 97

Oldest sediment cored:
Depth sub-bottom (m): 33.8
Nature: Foraminifer nannofossil ooze
Age: 270–440 × 10^3 y.
Measured seismic velocity: MnO: 2.22; Granular green clay: 1.72; Pelagic sediment: 1.51

Principal results: Hole 509B, located on a mound, is composed essentially of two sediment types: an upper unit of green "hydrothermal" clay with interbedded pelagic ooze (3–16 m) and a lower unit of pelagic ooze (16–33.4 m). The siliceous component within the oozes is essentially nil below 7 meters sub-bottom. Manganese-oxide fragments are present in the top 4.3 meters, mainly from 1.3–2.7 meters sub-bottom. The stratigraphic relationships between these units are the same as those found at Sites 506 and 507 except for the large amounts of manganese-oxide crust found at Hole 509B. Heat-flow measurements and pore-water sampling were conducted at Holes 509C and 509D.

BACKGROUND AND OBJECTIVES

Site 509 is centered in a mounds field, located at 0°35.30′S latitude and 86°07.90′W longitude, 21 to 22 km south of the Galapagos Spreading Center, and 4 km west of the north–south line passing through Sites 506 and 507 (Fig. 1). Site 509 coincides with IPOD Leg 54, Site 424; Holes 509 and 509B are located, respectively, off and on a mound about 400 ft. and 600 ft. west and slightly north of Hole 424A. The sediment cover is about 32 to 34 meters thick, and the underlying basement is assumed to be 0.60 to 0.63 m.y. old on the basis

---

[1] Honnorez, J., Von Herzen, R. P., et al., *Init. Repts. DSDP*, 70: Washington (U.S. Govt. Printing Office).

[2] Jose Honnorez (Co-Chief Scientist), Rosenstiel School of Marine and Atmospheric Sciences, University of Miami, Miami, Florida; Richard P. Von Herzen (Co-Chief Scientist), Woods Hole Oceanographic Institution, Woods Hole, Massachusetts; Timothy J. Barrett, Mineralogisches Institut, Universitat Tübingen, Tübingen, Federal Republic of Germany (present address: University of Toronto, Toronto, Ontario, Canada); Keir Becker, Marine Physical Laboratory, Scripps Institution of Oceanography, La Jolla, California; Michael L. Bender, Graduate School of Oceanography, University of Rhode Island, Kingston, Rhode Island; Peter E. Borella, Deep Sea Drilling Project, Scripps Institution of Oceanography, La Jolla, California (present address: Saddleback College, Mission Viejo, California); Hans-Wolfgang Hubberten, Institut für Petrographie und Geochemie der Universität Karlsruhe, Federal Republic of Germany; Steven C. Jones, Department of Geology, Florida State University, Tallahassee, Florida (present address: Mobil Oil Company, New Orleans, Louisiana); Shun-ichiro Karato, Ocean Research Institute, University of Tokyo, Tokyo, Japan (present address: The Australian National University, Canberra, Australia); Christine Laverne, Laboratoire de Geologie, Université de l'Ocean Indian, Ste. Clothilde, Réunion, France; Shaul Levi, School of Oceanography, Oregon State University, Corvallis, Oregon; Areg A. Migdisov, Vernadsky Institute of Geochemistry and Analytical Chemistry, USSR Academy of Sciences, Moscow, USSR; S. Anthony Moorby, Department of Geology, Imperial College, London, United Kingdom; Ed L. Schrader, Department of Geology and Geography, University of Alabama, University, Alabama (present address: J. M. Huber Corporation, Macon, Georgia).

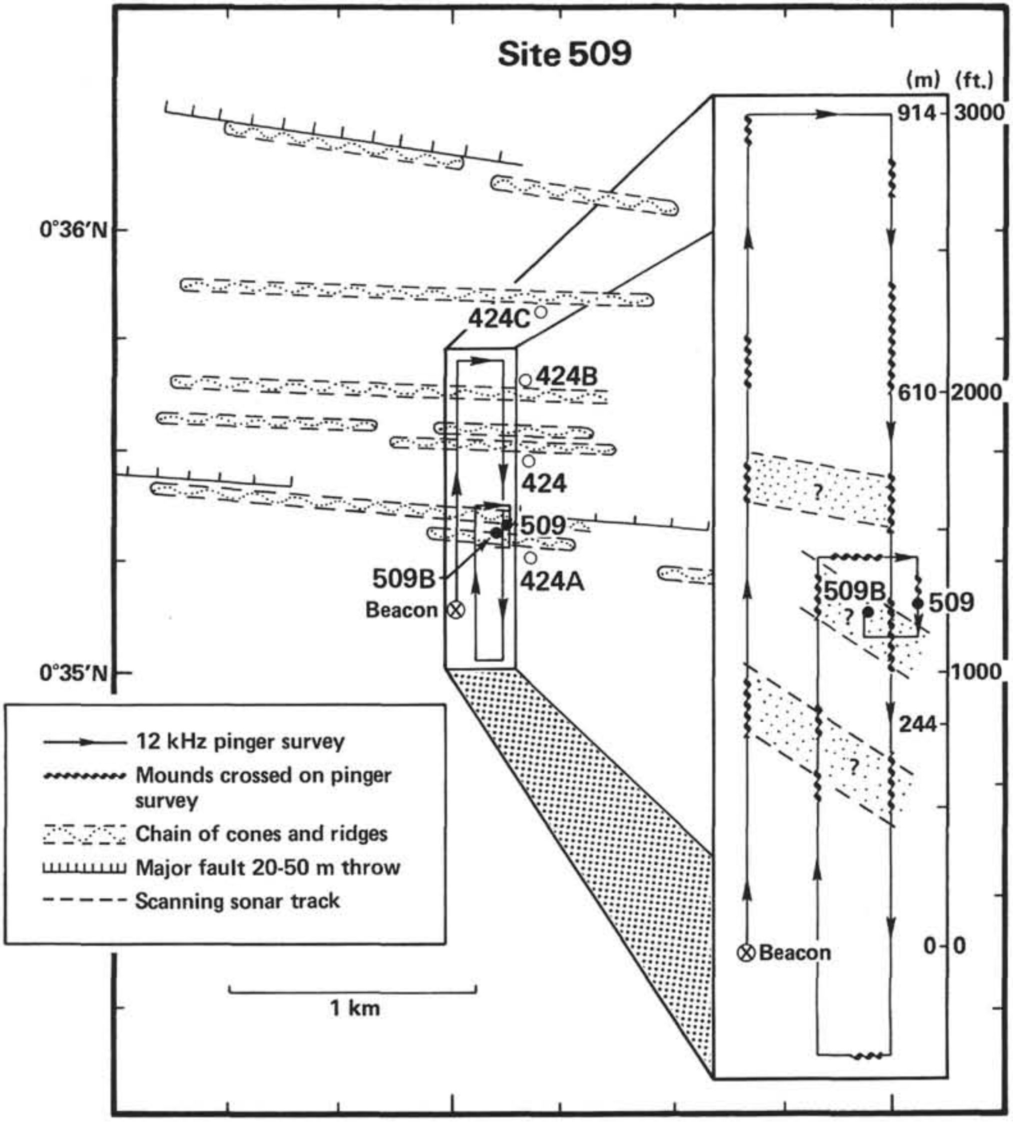

Figure 1. Detailed mound site survey, Site 509.

of the 3.5 cm/y. half-spreading rate inferred from the magnetic anomalies.

Our objectives were the same as for these two sites, but emphasis was placed on complementing and improving Leg 54 sediment recovery and, therefore, the stratigraphy and regional extension of its various lithological types (see general introduction to the first part of Leg 70). We were particularly concerned with the following questions raised by the published results of the Leg 54 scientific party:

1) What is the actual lithological sequence in the mounds of this field, and how does this sequence compare to those of the other two mounds fields that had already been studied during this leg?

2) Do hydrothermal layers exist in the sedimentary column between adjacent mounds?

In fact, we already knew that the hydrothermal clays do not extend far from the mounds, because, at the non-mound Site 508 no such material was present in the exclusively pelagic sediment column. We also knew from the coring of other off-mound holes on this leg that the hydrothermal material did not even exist between mounds areas. But it seemed important to confirm that the mounds field studied during Leg 54 was not different from the other two we had investigated.

OPERATIONS

Site 509 (Fig. 1) is located in the same mounds area as Site 424, which was drilled on Leg 54, and about 6 km NNW of Site 508. The approach to Site 509 came at an awkward time in that no satellite navigation fixes were obtained, so that the navigation was entirely dead-reckoned. Upon nearing the site of the intended beacon drop, we determined from the detailed U.S. Navy bathymetry chart that we had not covered the expected bathymetric profile. Therefore, the vessel was hove to without dropping the beacon to await the next satellite fix about one hour later. This showed us to be about 2 km to the north of our intended site, and the positioning was corrected by dead reckoning. A beacon was dropped at 0012 hours (local time) on Nov. 27. The drill string was lowered, equipped for hydraulic piston coring. A detailed survey to locate the mounds was conducted from 0942 to 1500 hr. using the 12-kHz pinger (Fig. 1). A bottom-reflecting 12-kHz pinger was attached to the drill string approximately 102 meters above the bit. The criteria used to identify the mounds are the same as those discussed in the Sites 506 and 507 Operations reports. Five holes were drilled. Their offset positions relative to the beacon and spud-in times are listed below.

Hole	Offset Position (feet from beacon)	Spud-in Time (hr)
509	1250 N, 600 E	1538 (Nov. 27)
509A	1250 N, 600 E	0007 (Nov. 27)
509B	1200 N, 400 E	0339 (Nov. 28)
509C	1200 N, 400 E	1042 (Nov. 28)
509D	1400 N, 600 E	1309 (Nov. 28)

Although initially we attempted to locate Hole 509 over a mound, the nature of sediment recovered and hindsight indicated that it was located just off a mounds site. Sediment was cored to the basement (32.3 m) with 100% recovery. We wanted to determine the lateral extent of the "hydrothermal" sediments. A heat-flow measurement and pore-water sample were attempted in Hole 509A. The pore-water sampler malfunctioned, possibly as a result of having free-fallen. Hole 509B was drilled on a mound. Sediments were cored to the basement with the hydraulic piston corer (33.8 m cored, 96.5% recovery). In Holes 509C and 509D heat-flow measurements and pore-water samples were taken on and off a mound, respectively. The instrumentation was lowered on the sandline and measurements were made at 2713, 2722, and 2731 meters below the rig floor; water samples were taken at 2722–2731 meters. Seafloor depths at these sites were 2702 and 2708 meters below the rig floor, respectively.

Upon completion of the final experiments, the drill pipe was pulled and at 2048 hours (November 28) the *Glomar Challenger* started steaming to Site 510.

SEDIMENT LITHOLOGY AND STRATIGRAPHY

Hole 509

Hole 509 was drilled off a mound (Table 1). The drill penetrated 32 meters of siliceous foraminifer nannofossil ooze before encountering basement. The uppermost 20 cm of sediment recovered were brown pelagic ooze (Fig. 2). Green hydrothermal clay and Mn-oxide fragments are not found in this hole. The major and minor constituents of the sediments, determined from smear slides, are: nannofossils 30–80%, foraminifers 2–20%, diatoms tr.–25%, radiolarians tr.–15%, silicoflagellates tr.–5%, sponge spicules tr.–3%. Well-preserved Zoophycus, Planolites(?), and halo burrows are present. A 3-cm thick layer of colorless volcanic ash is present in Sample 509-4-2, 64–67 cm.

Table 1. Coring summary, Site 509.

Core	Date	Time	Depth from Drill Floor (m) Top Bottom	Depth below Seafloor (m) Top Bottom	Length Cored (m)	Length Recovered (m)	Recovered (%)
Hole 509							
1	11/27/79	1556	2704.4–2405.4	0.0–1.0	1.0	1.15	100
2	11/27/79	1646	2705.4–2709.8	1.0–5.4	4.4	4.51	100
3	11/27/79	1740	2709.8–2714.2	5.4–9.8	4.4	4.53	100
4	11/27/79	1831	2714.2–2718.6	9.8–14.2	4.4	4.57	100
5	11/27/79	1925	2718.6–2723.0	14.2–18.6	4.4	4.46	100
6	11/27/79	2023	2723.0–2727.4	18.6–23.0	4.4	4.53	100
7	11/27/79	2108	2727.4–2731.8	23.0–27.4	4.4	4.46	100
8	11/27/79	2157	2731.8–2736.2	27.4–31.8	4.4	4.32	98
10	11/27/79	2303	2736.2–2736.7	31.8–32.5	0.5	0.08	16
				Total:	32.3	32.61	
Hole 509B							
1	11/28/79	0400	2701.8–2704.8	0.0–3.0	3.0	3.1	100
2	11/28/79	0454	2704.8–2709.2	3.0–7.4	4.4	4.39	100
3	11/28/79	0546	2709.2–2713.6	7.4–11.8	4.4	3.91	89
4	11/28/79	0637	2713.6–2718.0	11.8–16.2	4.4	4.20	95
5	11/28/79	0731	2718.0–2722.4	16.2–20.6	4.4	4.09	93
6	11/28/79	0823	2722.4–2726.8	20.6–25.0	4.4	4.52	100
7	11/28/79	0923	2726.8–2731.2	25.0–29.4	4.4	4.34	99
8	11/28/79	1017	2731.2–2735.6	29.4–33.8	4.4	4.08	93
				Total:	33.8	32.63	

Hole 509B

The drill at Hole 509B, located on a mound (Table 1), penetrated 33.4 meters of sediment before encountering basement (Fig. 2). As at Sites 506 and 507, two main lithological units can be distinguished: an upper unit of green hydrothermal clay with interbedded pelagic ooze (3–16 m sub-bottom) and a lower unit of pelagic ooze only (16–33.4 m). Mn-oxide fragments also occur in the uppermost 4.3 meters, mainly from 1.3 to 2.7 meters in Core 1, Section 1.

Mn-oxide fragments and granular green clay are also present in the top 10 to 80 cm of all underlying cores (Cores 2–8). These probably represent loose fragments from the top of the section which have fallen down the hole during core retrieval.

Taking into account the presence of the coring breccias and void spaces within the cores, the actual thickness of recovered sediment is reduced to 13.7 meters for the upper unit of green hydrothermal clays with interbedded pelagics and 14.4 meters for the lower unit of pelagic ooze.

A notable feature of Hole 509B is the enrichment of Mn oxides in its upper 4 meters. The Mn oxide occurs as fragments in Core 1 and as microaggregates dispersed in variable amounts through the pelagic oozes within Cores 1 and 2, Section 1. Fe-oxides, tentatively identified in smear slides and by color changes, occur as fine-grained aggregates which are present (1) together with Mn microaggregates in the pelagic oozes, leading to a dark olive green to olive brown coloration, and (2) in granular clay intervals within the upper 6 meters of the sediment column, producing a dusky yellow brown coloration.

At Hole 509B, an unusual minor unit occurs which was not observed at other mounds sites. It consists of a dark brownish black ooze comprising black oxides (approximately 60–70%), orange brown Fe-oxides (approximately 20–30%), and siliceous microfossils (approximately 10%). Calcareous microfossils are absent. This material forms two beds of 5 to 10 cm thickness, one in

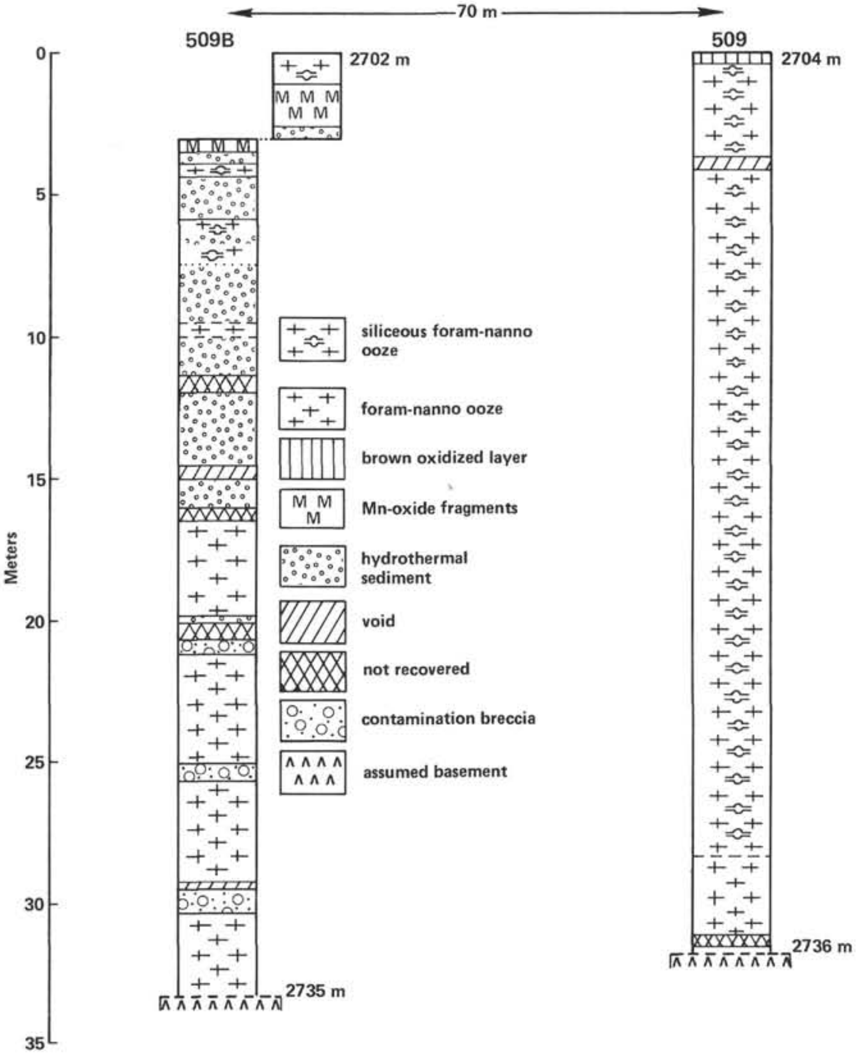

Figure 2. Lithologic column, Site 509.

Core 1, Section 1 and the other in Core 2, Section 1. Horizontal plates of Mn crust, up to 2 × 2 × 0.5 cm in size, separated by 5 to 15 cm intervals, occur within the olive pelagic ooze interval in the middle of Core 2, Section 1. Another unusual occurrence is concretion-like nodules up to 3 × 2 × 2 cm in size, consisting of Mn-oxide fragments and green clay granules within the light gray green pelagic ooze interval in Core 2, Section 3. Contacts between green hydrothermal clay intervals and pelagic ooze intervals are mainly gradational over 10 to 20 cm.

Within the interbedded green clay and pelagic sediments, the abundance of siliceous microfossils decreases from 10 to 30% in the upper 8 meters, to a few percent or less in sediments below 8 meters. The main pelagic ooze unit, which extends from 16 meters sub-bottom to basement at 33.4 meters, consists almost entirely of foraminifer nannofossil ooze with less than 5% of siliceous microfossils. In the lowermost 3 meters of pelagic ooze, immediately overlying basement, small (<3 mm) basalt shards are present.

X-RAY DIFFRACTION ANALYSIS

The same sample preparation techniques were followed as were used at previous sites. The results are summarized in Table 2.

Calcite is the dominant mineral identified in all the pelagic ooze samples and in the mixed ooze and green clay sample from Core 6, Section 2.

All six samples of green hydrothermal clay showed one or more nontronite peaks. A sample of Mn-oxide crust (Sample 509B-1-2, 70–71 cm) contained some nontronite, but the main mineral identified is todorokite.

SEDIMENTATION RATES

A summary of sedimentation and accumulation rates is given in Table 3. As compared to Sites 506–508 the sedimentation and accumulation rates at Site 509 are very similar. Similar sedimentation and accumulation rate of mounds and off-mounds sediments are attributed to their dissolution by hydrothermal solutions and replacement by hydrothermal products.

Table 2. X-ray diffraction analysis, Site 509.

Sample (interval in cm)	Mineral	Major Peak 2θ	(Uncorr.) d(Å)	Major Peak 2θ	(Corr.) d(Å)
509-1-1, 31–33	Calcite	38.8	2.32	40.0	2.25
(Off-mounds brown pelagic ooze)	Calcite	35.5	2.53	35.7	2.51
	Calcite	28.9	3.09	29.1	3.07
		27.4	3.25	27.6	3.23
		25.25	3.52	25.45	3.50
	Nontronite	7.75	11.4	7.95	11.1
	Nontronite	7.3	12.1	7.5	11.8
509-2-3, 39–39	Calcite	39.2	2.30	39.4	2.29
(Pelagic ooze–nanno-ooze)	Calcite	35.75	3.51	35.95	2.50
	Halite	31.5	2.84	31.7	2.82
	Halite	31.2	2.87	31.4	2.85
	Calcite	29.2	3.06	29.4	3.04
	Sylvite	28.15	3.17	28.35	3.15
	(internal std.)				
	Calcite	22.8	3.90	23.0	3.87
509-3,CC (5–7)	Calcite	39.2	2.30	39.4	2.29
(Pelagic ooze)	Calcite	35.7	2.51	35.9	2.50
	Halite	31.4	2.85	31.6	2.83
	Calcite	29.1	3.07	29.3	3.05
	Sylvite	28.0	3.19	28.2	3.16
	(internal std.)				
	Calcite	22.75	3.91	22.95	3.88
509-4-2, 67–68	Sylvite	28.15	3.17	28.35	3.15
(Pelagic ooze)	(internal std.)				
509-5,CC (8–9)	Calcite	39.2	2.30	39.4	2.29
	Calcite	35.7	2.51	35.9	2.50
	Halite	31.5	2.84	31.7	2.82
	Halite	31.25	2.86	31.45	2.84
	Calcite	29.2	3.06	29.4	3.04
	Sylvite	28.15	3.17	28.35	3.15
	(internal std.)				
	Calcite	22.8	3.90	23.0	3.87
	Nontronite?	6.2	14.3	6.4	13.8
509-6-2, 20–21	Calcite	39.2	2.30	39.4	2.29
(Pelagic ooze with	Calcite	35.75	2.51	35.95	2.50
dark green clay?)	Halite	31.25	2.86	31.45	2.84
	Calcite	29.1	3.07	29.3	3.05
	Calcite	22.8	3.90	23.0	3.87
		21.5 br.	4.13	21.7	4.09
		10.0?	8.85	10.2	8.67
		10.2?	8.67	10.4	8.51
509B-1-2, 70–71		22.1	4.02	22.3	3.99
(Mounds—Mn-oxide crust)	Todorokite	17.9 br.	4.96	18.1	4.90
		16.45	5.40	16.65	5.32
	Todorokite	8.7	10.2	8.9	9.94
	Nontronite	7.7 br.	11.5	7.9	11.2
	Nontronite	6.5 v. br.	13.6	6.7	13.2
509B-1-2, 143–144		36.3	2.47	36.5	2.46
(Greenish yellow clay		34.2	2.62	34.4	2.61
"hydrothermal"?)	Sylvite	28.15	3.17	28.35	3.15
	(internal std.)	21.5	4.13	21.7	4.09
		20.0	4.44	20.2	4.40
		19.0	4.67	19.2	4.62
	Nontronite	7.75 br.	11.4	7.95	11.1
	Nontronite	6.4 v. br.	13.8	6.6	13.4
509B-2-1, 139–140	Sylvite	28.1	3.17	28.3	3.15
(Greenish yellow granular clay)	(internal std.)				
	Nontronite	20.0	4.44	20.2	4.40
		12.9	6.86	13.1	6.76
		8.1	10.9	8.3	10.7
	Nontronite	7.7	11.5	7.9	11.2
	Nontronite	6.7	13.2	6.9	12.8
509B-2-2, 40–41	Sylvite	28.1	3.17	28.3	3.15
(Mixed green clay	(internal std.)	19.3	4.60	19.5	4.55
w/lighter material)	Nontronite	17.5	5.07	17.7	5.01
		13.25	6.70	13.45	6.58
	Nontronite	7.7	11.5	7.9	11.2
	Nontronite	6.4 v. br.	13.8	6.6	13.4
509B-4-1, 68–69		34.4	2.61	34.6	2.59
(Green clay granular)	Halite	31.45	2.84	31.65	2.82
	Nontronite	19.35	4.58	19.55	4.54
		13.8	6.42	14.0	6.33
	Nontronite	7.8 br.	11.3	8.0	11.1
	Nontronite	6.6 v. br.	13.4	6.8	13.0
509B-4-1, 95–96	Nontronite	7.8 br.	11.3	8.0	11.1
(Green clay w/yellow	Nontronite	7.0	12.6	7.2	12.3
granular clay)	Montmorillonite?	6.3 v. br.	14.0	6.5	13.6
	Montmorillonite?	5.3	16.7	5.5	16.1
509B-4-2, 43–49		13.5	6.56	13.7	6.46
(Green clay)		8.8	10.0	9.0	9.83
	Nontronite	7.75	11.4	7.95	11.1
	Montmorillonite?	6.6 v. br.	13.4	6.8	13.0

Note: br. = broad; v. br. = very broad.

PORE-WATER GEOCHEMISTRY

Site 509 Results

Site 509 pore waters (Tables 4–6; Fig. 3) show the features common to mounds area samples (i.e., those from Sites 506, 507, and 509). NH_3 in both holes is lower than in the low heat-flow site, Site 508. It is lowest but nearly constant in the mounds hole (Hole 509B), and it decreases with depth, reflecting slow upward convection in the off-mounds sediments and more rapid convection through the mounds. The pore waters are enriched in Ca by 0.5 to 2.0 mM and depleted in Mg by 1 to 3 mM, presumably as a result of reactions in basement. Si concentrations in the off-mound hole (Hole 509) are typical for pelagic sediments, while those in the mounds hole are lower and highly variable.

"Runoff" samples were taken at Hole 509B. These samples were collected by letting water from the mounds

Table 3. Sedimentation rates, Site 509.

Hole	S^a	Sedimentation Rate (cm/10^3 y.)		P^b (%)	Sediment Accumulation Rate (cm/10^3 y.)		Average Grain Density (g/cm^3)	Accumulation Rates (g/cm^2/ 10^3y.)	
		A	B		A	B		A	B
509	32.3	7.34	5.38	82.5	1.30	0.96	2.67	3.48	2.56
(off-mound)		11.9			2.12			5.66	
509B	33.8	7.5	5.5	83.3	1.25	0.92	2.81	3.51	2.59
(mound)		12.22			2.04			5.73	

Note: Sedimentation accumulation rate = [(1 − *P*) × sediment thickness/*t*], where *t* = time. Accumulation rate = sedimentation accumulation rate × average grain density. Columns lettered "A" show minimum and maximum values based on paleontological evidence. Paleontological evidence estimates the age at the bottom of each hole to be 270–440 × 10^3 y. Columns lettered "B" are values based on spreading rates taken from Klitgord and Mudie (1974). Spreading rate estimates assign an age of approximately 540 × 10^3 y. for the ocean crust in the area.

[a] *S* = Sediment thickness (recorded drilling thickness).

[b] *P* = Porosity (fraction void space) = (void space)/(total volume); values are averages taken from the Physical Properties section.

Table 4. Shipboard pore-water data, Holes 509, 509B.

Core-Section	ISPW No.	Sub-bottom Depth (m)	SiO_2 (μM)	NH_3 (μM)	Ca^{2+} (mM)	Mg^{2+} (mM)	Cl (‰)	S (‰)
Hole 509								
2-1	122	2.40–2.50	640	35	12.291	51.54	20.06	35.8
2-2	123	3.59–3.70						
2-3	124	5.39–5.50	590	27	12.249	51.71	19.46	35.5
3-1	125	6.79–6.90	630	27				
3-2	126	8.29–8.40	660	22				
3-3	127	9.72–9.83	620	22	12.060	51.47	19.52	35.5
4-1	128	11.19–11.30						
4-2	129	12.69–12.80	510	11				
4-3	130	13.97–14.08	530	10	12.123	50.93	19.29	35.2
5-1	131	15.59–15.69						
5-2	132	17.09–17.20	550	10				
5-3	133	18.38–18.49	520	9	12.102	51.55	19.49	34.9
6-1	134	19.99–20.10	550	10				
6-2	135	21.49–21.60	540	9	11.410	52.18	19.29	35.2
7-1	136	24.39–24.50						
7-2	137	25.89–26.00	510	6				
7-3	138	27.25–27.36	510	9	11.33	51.37	19.19	35.2
8-1	139	28.79–28.90	470	5				
8-2	140	29.99–30.10	470	5	11.221	51.48	18.86	35.2
8-3	141	31.51–31.61	310	14				
Hole 509B								
2-1	142	4.39–4.50	390	8				
2-2	143	5.89–6.00	390	7	12.27	51.31	19.13	35.2
2-3	144	7.39–7.50	350					
3-2	145	10.29–10.40	330	4	12.08	51.52	19.16	34.6
4-3	146	15.80–15.91	260		12.27	51.16	19.13	34.6
5-1	147	17.59–17.70	390	6	11.81	51.39	19.09	35.8
5-2	148	19.09–19.20	300	6				
5-3	149	20.05–20.16	120					
6-1	150	21.99–22.10	470		11.79	51.17	19.26	35.2
6-2	151	23.49–23.60	470	4				
6-3	152	24.89–25.00	450		11.52	51.56	18.99	35.5
7-1	153	26.39–26.50	470	4				
7-2	154	27.89–28.00						
7-3	155	29.08–29.19	420	7	11.18	51.20	19.06	36.3
8-3	156	33.24–33.35	450		11.39	50.87	19.06	37.4

Table 5. Shipboard pore-water data for run-off samples, Hole 509.

Core-Section	Sub-bottom Depth (m)	SiO_2 (μM)	Ca^{2+} (mM)	Mg^{2+} (mM)	Cl (‰)	S (‰)
1-1 (bottom) 1W118	1.50	410	12.29	50.67	19.13	34.9
3-1 (bottom) 1W119	8.90	390	12.35	51.31	19.26	34.9
3-2 (bottom) 1W120	10.40	350	12.19	51.36	18.99	34.4
4-2 (top) 1W121	13.3	410	12.44	51.58	19.03	34.4

Table 6. Shipboard pore-water data for *in situ* samples, Site 509.

Sample	Sub-bottom Depth (m)	SiO_2 (μM)	Ca^{2+} (mM)	Mg^{2+} (mM)	Cl (‰)	S (‰)
Hole 509C						
IW156		360	11.05	50.04	18.40	33.6
ISPW #12	Z = 24 ± 2	380 corrected to S = 19.2	11.53	52.22	19.2	
Hole 509D						
IW157		220	10.61	49.95	18.43	33.6
ISPW #13		230	11.07	52.12	19.2	

gravels flow into a beaker when sections were cut on the catwalk, and subsequently filtering the water through 0.45 μm filters. The chemistry of these samples (see Table 5) is in good agreement with that of nearby squeeze samples.

Two *in situ* samples were collected. Both had salinities close to the surface water value, but they were enriched in Ca, Mg, and Si with respect to surface water, and enriched in Ca and depleted in Mg with respect to deep water. These samples thus clearly contain a large component of pore water. To quantitatively interpret the results, we make the working assumption that the samples are entirely free of surface water contamination and that the low salinities are solely the result of contamination from fresh water initially filling the stainless steel coil of the *in situ* sampler. The concentrations of Ca, Mg, and Si are thus corrected for dilution by multiplying by a factor of 1.04 (determined from the ratio of the measured chlorinity for these samples to that for centrifuged pore waters). The corrected Ca and Si results for Hole 509 differ greatly from the chemistry of centrifuge samples. The data for this sample can be largely reconciled with the assumption that the sample is an equal mixture of true pore water and surface water pumped downhole. On the other hand, we cannot exclude the possibility that the sample is composed entirely of true pore water and differs from Hole 509 centrifuge samples because of either local variability in pore-water chemistry or a very serious artifact in centrifuge sampling.

The chemistry of the mounds *in situ* sample (at Hole 509B) is in excellent agreement with that of the nearby centrifuge sample. There is a silica anomaly of about 15%, which may reflect a centrifuge temperature a few degrees higher than the *in situ* temperature.

A most intriguing result is the high salinity of the basal pore waters at Hole 509B. At present we have no idea about the significance of this result.

Synthesis of Pore-Water Data from Sites 506–509

In the following discussion we first examine evidence for the integrity of the pore-water samples. We then discuss the implications of our data for pore-water geochemistry at Sites 506 to 509. The key conclusion is that mounds and off-mounds sediments are flooded by upward-flowing seawater that has reacted with basalt and

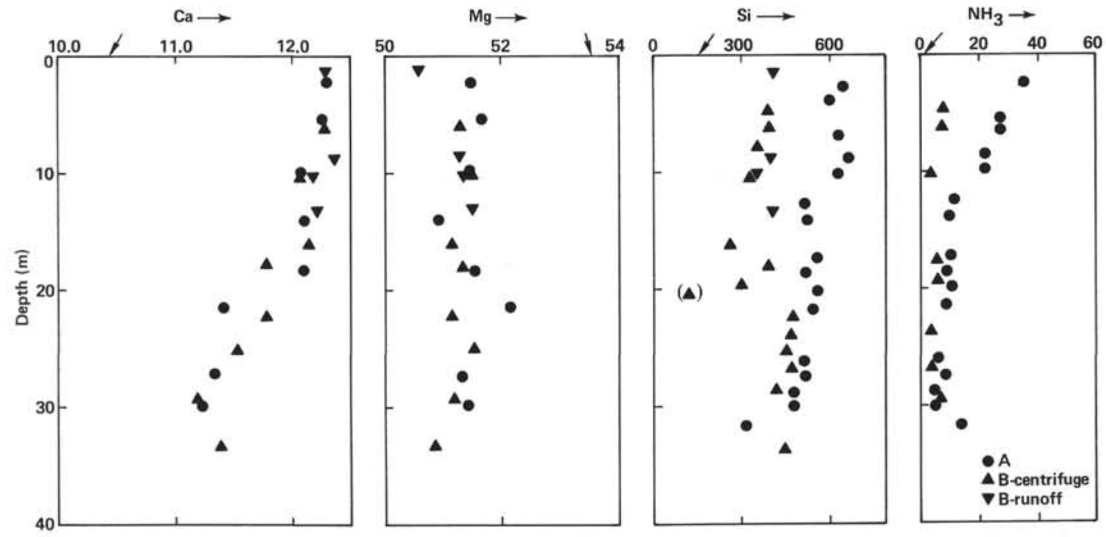

Figure 3. Site 509 pore-water chemistry. (Ca and Mg in mM/kg, Si and NH in μM/kg. Arrows indicate bottom water concentrations.)

is accordingly enriched in Ca and depleted in Mg relative to bottom seawater.

Sample Integrity

It is important to examine sample integrity, because pore-water chemistry differs little from that of bottom water. One line of evidence involves comparing *in situ* and centrifuged samples. The raw data are compared in Table 7 and Figure 4, and the differences summarized in Table 8. When all results are considered, there are large differences between centrifuged and *in situ* data: the standard deviation of the difference (twice the standard deviation from the mean) is ±0.6 mM for Ca, ±1 mM for Mg, and ±140 μM for Si. These differences far exceed experimental error. If we restrict the comparison by eliminating the samples showing serious disagreement in Mg (Hole 508) and Si (Hole 509) on the grounds that they may record local variability (and in the case of Hole 509, surface water contamination), we end up with a systematic Ca difference of −0.4 mM, and no systematic differences and small variability in Mg and Si data. The situation improves slightly when we restrict the comparison to Site 510 samples (those least likely to be affected by local variability). The conclusion is that centrifuge Ca data are systematically low by about 0.5 mM, centrifuge Mg data are satisfactory, and centrifuge Si data show no systematic offset but are slightly compromised by an inherent sampling artifact of ±10%. The origin of the Si artifact is not understood.

Table 7. Synthesis of pore-water chemistry of *in situ* and centrifuge results, Sites 506–509.[a]

Hole	ISPW No.	Ca^{2+} (mM)	Mg^{2+} (mM)	Si (μM)
Hole 506B				
Centrifuge (15 m)		11.6	51.7	390
in situ	3	12.2	51.4	540
Hole 508				
Centrifuge (16 m)		10.3	52.8	640
in situ	8	10.2	53.0	660
Centrifuge (25 m)		10.2	53.0	660
in situ	10	11.0	51.6	720
Hole 509				
Centrifuge (18 m)		11.9	51.6	503
in situ	13	11.1	52.1	230[b]
Hole 509B				
Centrifuge (24 m)		11.6	51.4	460
in situ	12	11.5	52.2	380[b]

[a] "Centrifuge" obtained from plots by interpolation.

[b] Surface-water contamination.

Geographical Variations in Pore-Water Chemistry

Next we examine data for evidence of differences in pore-water chemistry from hole to hole. In Figure 5, Mg is plotted vs. Ca for each hole. The most obvious result (see summary in Table 9) is that all high heat-flow samples are enriched in Ca and depleted in Mg relative to bottom water. By contrast, centrifuge samples from the low heat-flow site (Hole 508) have no Ca enrichment and a smaller Mg depletion than the high heat-flow samples. These results support the general view that the sediments from mounds and surrounding areas with high heat flow are sites of upward convection of water which has exchanged with the basement, whereas the low heat-flow site (Hole 508) is one of recharge.

There are several intriguing aspects to the data from Site 508. First, the samples show a Mg depletion of 0.6 mM (1%) relative to bottom water. This depletion may reflect a sampling artifact, *in situ* inorganic reactions in the sediments as recorded elsewhere, Mg substitution for detrital Fe resulting from anoxic diagenesis as described by Drever (1971), or the presence of a small amount of formation water in the sediments. The second result to be considered is the Ca data above 30 meters. These average out to a value about 0.2 mM below the bottom water concentration, but, when corrected for the sampling artifact, fall 0.3 mM above the bottom water value. This result can very nearly be ex-

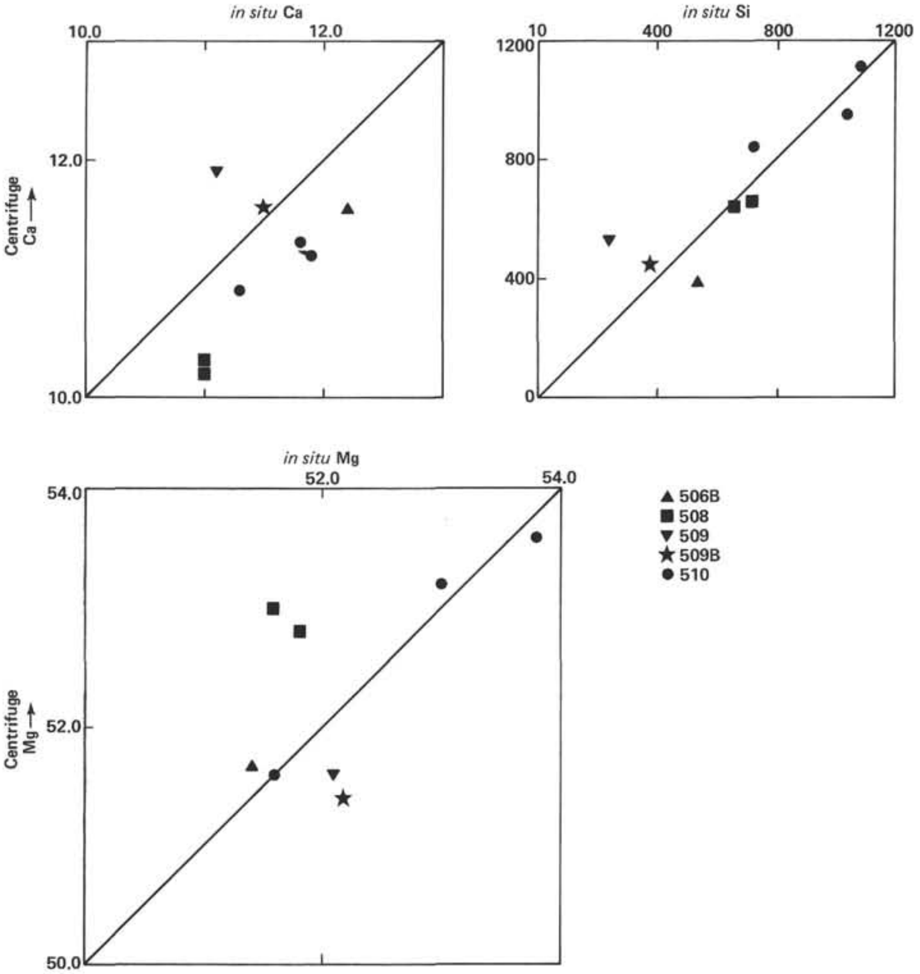

Figure 4. Comparison of centrifuge sample and *in situ* sample Ca, Mg, and Si concentrations for Leg 70 pore-water samples (lines are 1:1).

Table 8. Differences in Ca, Mg, and Si concentrations of *in situ* and centrifuge samples.[a]

	Ca (mM)		Mg (mM)		Si (μm)	
	Centrifuge *in situ*	Std. Dev.	Centrifuge *in situ*	Std. Dev.	Centrifuge *in situ*	Std. Dev.
All samples (n = 8)	−0.4	±0.3	+0.2	±0.5	−50	±70
All samples except those from Holes 508 and 509 (n = 5)	−0.4	±0.2	−0.1	±0.2	−10 (0%)	±50 (±9%)
Hole 510 samples	−0.5	±0.1	0	±0.1	10 (2%)	50 (±10%)

[a] Calculated from data, Table 4.

plained by assuming downwelling of bottom water and a diagenetic Ca enrichment of about 0.15 mM, resulting from metabolic CO_2 production during O_2 reduction and subsequent calcite dissolution. The high Ca and low Mg concentrations of pore waters in basal sediments at Site 508 and 508 *in situ* samples are a third puzzling feature (see Fig. 4 in Site 508 pore-water summary). The high Ca concentration in samples at 33 and 35 meters at Hole 508 may be interpreted as reflecting diffusive exchange with underlying Ca-rich and Mg-poor formation waters. This interpretation implies a recharge rate of about 0.5 cm/y.) The *in situ* results (Site 508 summary), which show high Ca and low Mg concentrations in samples at 17 and 26 meters, cannot be so interpreted: They represent the presence of formation waters too high up in the sedimentary column to be explained by upward diffusion against recharge at the recharge rates inferred from the temperature data. Perhaps the least unsatisfactory explanation is that in the low heat-flow area there is a complex circulation pattern involving some local upwelling of basement waters. The heat-flow data suggest that there is variability in flow on a small

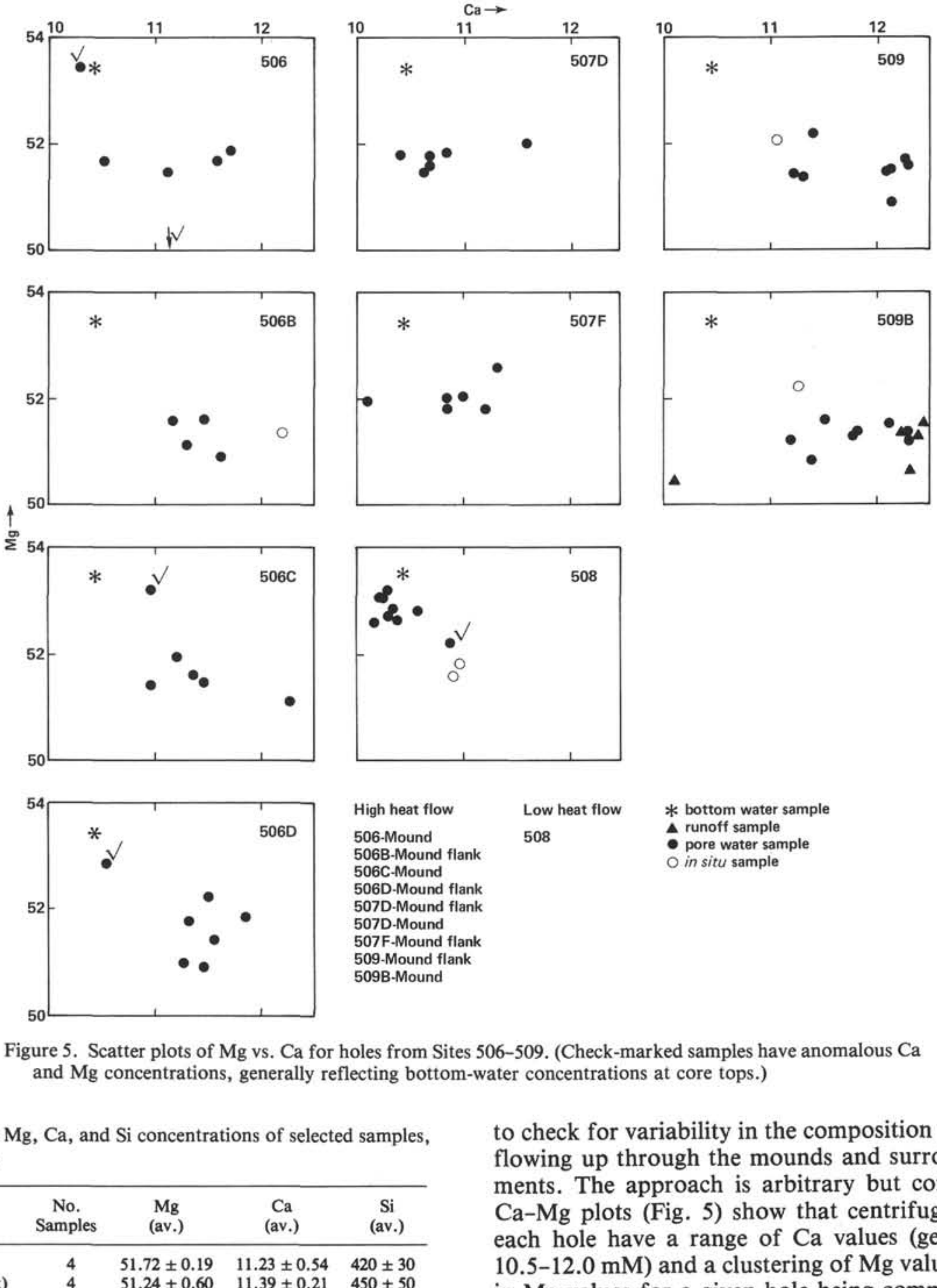

Figure 5. Scatter plots of Mg vs. Ca for holes from Sites 506–509. (Check-marked samples have anomalous Ca and Mg concentrations, generally reflecting bottom-water concentrations at core tops.)

Table 9. Average Mg, Ca, and Si concentrations of selected samples, Sites 506–509.

Hole	No. Samples	Mg (av.)	Ca (av.)	Si (av.)
506 (mound)	4	51.72 ± 0.19	11.23 ± 0.54	420 ± 30
506B (mound flank)	4	51.24 ± 0.60	11.39 ± 0.21	450 ± 50
506C (mound)	5	51.51 ± 0.28	11.50 ± 0.49	460 ± 140
506D (mound flank)	6	51.55 ± 0.52	11.50 ± 0.21	510 ± 20
507D (mound)	6	51.73 ± 0.16	10.79 ± 0.40	320 ± 90
507F (mound flank)	6	52.01 ± 0.28	10.90 ± 0.43	460 ± 70
508 (low heat flow)	8	52.82 ± 0.49	10.32 ± 0.13	590 ± 90 (n = 7)
509 (mound flank)	8	51.53 ± 0.35	11.85 ± 0.45	530 ± 100
509B (mound)	12	51.26 ± 0.27	11.97 ± 0.42	390 ± 60
Bottom water		53.45	10.45	160

scale; but contrary to our pore-water data, all three sets of heat-flow measurements at Site 508 imply recharge only.

Returning now to the chemistry of pore-water samples from the high heat-flow areas, we examine the data to check for variability in the composition of the waters flowing up through the mounds and surrounding sediments. The approach is arbitrary but consistent. The Ca-Mg plots (Fig. 5) show that centrifuge samples at each hole have a range of Ca values (generally from 10.5-12.0 mM) and a clustering of Mg values (the range in Mg values for a given hole being comparable to the analytical error of about ±0.5%). We exclude the five samples (indicated by check marks in Fig. 5) which have Mg concentrations different from that of other samples in their respective holes, and calculate the average Mg, Ca, and Si concentrations for each hole of the other plotted centrifuge samples. The results are summarized in Table 7. The low heat-flow site is characterized by low Ca and high Mg relative to high heat-flow sites (discussed earlier) and high Si.

At a given mounds area site (i.e., at Sites 506, 507, and 509), the Ca and Mg concentrations in the different holes are indistinguishable, but there appear to be small differences in concentrations among the different sites.

For example, Site 507 has a Mg concentration 0.4 mM (0.8%) higher than that at 506 or 509. Site 507 has the lowest Ca concentration and Site 509 the highest. We are intrigued by the possibility that these variations may record small but significant differences in the composition of formation waters entering the sediment at the different sites.

Pore-Water SiO_2 Concentrations

The Si concentrations of pore water are higher in low heat-flow than in high heat-flow sediments. This result most likely reflects biogenic silica input close to the sediment-water interface. Descending waters (at Site 508) would receive this input as they start the trip down and would subsequently advect high Si waters down through the sediments. Ascending waters (at Sites 506, 507, and 509) would enter the sediment with the (unknown) formation-water Si content, gaining or losing on the way up, depending on the relative rates of Si input by biogenic silica dissolution and Si removal by clay mineral formation or absorption. In fact, Si generally increases toward the sediment/water interface in high heat-flow sites. This clearly is the case in Holes 506B and 509 and is suggested by high values near the top of Holes 506 and 507F. The implication is that formation water entering the sediment is relatively poor in silica. The fact that mounds samples generally have less Si than adjacent pelagic sections (Table 8) and that they sometimes have very low Si values (e.g., Holes 506C, 507D, 509B) constitute further evidence that the formation waters entering the sediment are silica-poor and gain biogenic Si as they ascend.

Thus, the pore-water data suggest that the formation waters under the high heat-flow area have lost Mg and gained Ca by reaction with basalt. According to the extensive Deep Sea Drilling Project pore-water data of McDuff and Gieskes (1976), such a change is the routine result of basalt alteration in the oceanic crust. The $\Delta Mg/\Delta Ca$ ratio is in the range of -1 to -2 (after correcting for artifacts in the centrifuge sample Ca data). Whether Si is gained or lost in the reaction cannot be estimated without knowing whether the formation waters originate from seawater which enters the basalt directly (in which case Si rises during the reaction from 160 to 200–400 μM) or by recharge through the sediment blanket (in which case Si falls from about 600 to 200–400 μM).

NH_3 Distribution in Pore Waters

NH_3 concentrations can be readily explained in terms of the simple models of convection. The source of ammonia is sulfate reduction of organic matter. Gravity core pore-water data have shown that O_2, NO_3, and MnO_2 are all consumed very close to the sediment-water interface, and Fe_2O_3 reduction is negligible. Hence SO_4 reduction and NH_3 production begin within the top meter or so of the sediment column. From the mounds data it is clear that the formation waters have negligible NH_3. Thus, the predicted NH_3 concentration variations are similar to those observed for Si—high throughout the low heat-flow site (because NH_3 is probably produced most rapidly in the top few meters) and low but increasing upward in the high heat-flow sites. The observations are in good agreement with predictions. At off-mounds sites, NH_3 increases towards the sediment/water interface. Concentrations within mounds are lower, either because they are flushed more rapidly or because less metabolic NH_3 is generated in them. NH_3 concentrations are highest at Site 508 (low heat flow), although concentrations increase more slowly than expected at shallow depths and decrease unexpectedly below 15 meters in the sediment. This latter decrease probably reflects incorporation into ion exchange sites of clay minerals.

PHYSICAL PROPERTIES

Three kinds of materials—pelagic sediments, green clays, and manganese oxides—were analyzed from this site.

The wet-bulk density of pelagic sediments ranges from 1.21 to 1.44 g/cm^3, porosity from 75 to 91%, sonic velocity 1.44 to 1.54 km/s, and thermal conductivity from 0.78 to 1.07 W/m•K. Manganese oxides have the highest wet-bulk density (1.59 to 2.28 g/cm^3), sonic velocity (1.94 to 2.47 km/s), and the lowest porosity (57.6 to 81.8%). Granular green clays have higher wet-bulk density (1.33 to 1.92 g/cm^3), sonic velocity (1.54 to 1.83 km/s), and average lower porosity (64 to 87%) and thermal conductivity (0.71 to 0.97 W/m•K) than the pelagic sediments.

The depth variation of physical properties is similar to that of previous sites.

HEAT FLOW

Two lowerings of the downhole temperature probe were made at Site 509, near each of the two hydraulic piston cores. Hole 509C, heat flow, was located near the mound core, Hole 509B; and Hole 509D, heat flow, was near the off-mound pelagic core, Hole 509. Unfortunately, each of the lowerings was marred by poor determination of at least one *in situ* temperature point of three, so the calculation and interpretation of sediment thermal gradients is not unequivocal. As at Sites 506–509, detailed thermal conductivity studies of the adjacent cores showed a strong linear increase of conductivity with depth (Karato and Becker, this volume; Becker et al., this volume).

Despite uncertainties in determining probe temperature, the temperature gradient at Hole 509C clearly decreases with depth. This is interpreted as indicating hydrothermal discharge near the mound at Hole 509B, at a rate of about 25 cm/y., with a surface heat flow of about 25 HFU. As at Site 506, the off-mound heat-flow measurement was linear with integrated thermal resistance, indicating conductive heat transfer of 10 HFU, and again indicating the localized nature of the hydrothermal processes in the sediments near the mounds. See Becker et al. (this volume) for a complete discussion of heat-flow results.

SEDIMENT PALEOMAGNETISM

Site 509 was located 21 to 22 km south of the Galapagos Spreading Center; its basement age is approximately 0.60 to 0.63×10^6 years, based on 3.5 cm/y. half-spreading rate as determined by Klitgord and Mudie (1974). The sediments at Site 509 were retrieved with the hydraulic piston corer, and reconnaissance paleomagnetic measurements were obtained on board the *Glomar Challenger* using the long vertical spinner magnetometer, described in more detail in the summaries of Sites 506 and 507. The measuring procedure at Site 509 was identical to that at Sites 506 and 507.

Hole 509 is composed entirely of foraminifer nannofossil ooze. Hole 509B, which is no more than 100 meters away from Hole 509, is composed of layers of Mn-oxide fragments, hydrothermal clays, and foraminifer nannofossil ooze. The preliminary paleomagnetic results are similar to those at Sites 506 and 507. One additional observation was that in Hole 509B, the Mn-oxide fragments composing Core 1, Section 2 exhibited unusually weak magnetization intensity, consistently less than 1×10^{-6} gauss, though the relative declinations were surprisingly well clustered. These low magnetization intensities are consistent with Leg 54 results, which showed that the Mn crusts are iron-poor. However, the relatively well-clustered relative declinations suggest that a small fraction of remanence-carry phase(s) is also present.

CONCLUSIONS

Site 509 is centered on a mounds field, located at 0°35.30′S latitude and 86°07.90′W longitude, 21 to 22 km south of the Galapagos Spreading Center, and 4 km west of the north–south line passing through Sites 506 and 507. Site 509 coincides with IPOD Leg 54, Site 424; Holes 509 and 509B are located, respectively, off and on a mound about 400 ft. and 600 ft. west and slightly north of Hole 424A. Three heat-flow measurements were carried out at the same locations. The sediment cover is about 32- to 34-meters thick, and the underlying basement is assumed to be 0.60 to 0.63 m.y. old on the basis of the 3.5 cm/y. half-spreading rate inferred from the magnetic anomalies.

The overall thickness and lithological sequence of the mound sedimentary column of Hole 509B is very similar to those of the other two mounds sites (Table 10), i.e., Sites 506 and 507. The stratigraphy observed in the 33.4 meters of sediments cored in Hole 509B consists, from top to bottom, of the following units:

1) About 4 meters of various interbedded lithologies, including manganese-oxyhydroxide crust fragments up to 2.5 cm in maximum diameter and mainly in one 1.4-meter thick layer, pelagic oozes, smectite granular clay, and Mn-Fe-oxide ooze;

2) About 12 meters of green clays interbedded with pelagic oozes;

3) 17.4 meters of mainly nonsiliceous foraminifer nannofossil ooze overlying the basaltic basement.

The sedimentary column cored in Hole 509, located probably on the edge of a mound, is made up exclusively of 31.9 meters of siliceous foraminifer nannofossil ooze. This observation demonstrates that the hydrothermal material has no regional extension at this site either and, therefore, could not explain the sub-bottom reflectors observed by Lonsdale (1977). The fossil assemblages present at Site 509 were essentially identical to those of the previous sites.

Table 10. Composition of hydrothermal sediments with interbedded pelagic oozes.

	Hole					
Composition	506[a]	506C[a]	506D[b]	507D[a]	507F[b]	509B[a]
Sediment recovered[c]	12.7	11.3	1.4	25.0	2.8	13.5
Pelagic ooze (PO)	~3.1	~2.3	~0.5	~9.5	~1.0	~4.3
Green clay (GC)	~9.6	~9.0	~0.9	~15.5	~1.8	~9.2
Ratio GC/PO	~3.1	~3.9	~1.8	~1.6	~1.8	~2.1
Ratio GC/Total Sediment Recovered	0.76	0.80	0.64	0.62	0.64	0.68
	Entire Section					
Sediment recovered[c]	21.2	29.3	29.7	34.9	30.8	27.8
Pelagic ooze (PO)	~11.2	~19.3	~29.0	~19.4	~29.0	~18.3
Green clay (GC)	~10.0	~10[d]	~0.7	~15.6[d]	~1.8	9.5[d]
Ratio GC/PO	~0.89	~0.52	~0.02	~0.80	~0.06	~0.52
Ratio GC/Total Sediment Recovered	~0.47	~0.34	~0.02	~0.44	~0.06	~0.34

[a] Mounds hole.

[b] Off-mounds hole.

[c] Calculated from SR = DT − CV − NR, where SR = sediment recovered, DT = drilled thickness, CV = core voids in top or bottom cores (resulting from original absence of sediment), and NR = not recovered (washed out).

[d] Includes thin green clay intercalations within main pelagic ooze unit.

Small enrichments in pore-water calcium and depletions in magnesium again imply a flow of formation waters through mounds area sediments. Ammonia concentrations are also low, especially in Hole 509B, suggesting rapid flushing by upward convection.

Heat flows were quite high in each hole of this site: about 500 and 700 mWm^{-2} at Holes 509 and 509B, respectively. Thermal gradients at Hole 509B decreased with depth, suggesting hydrothermal discharge through the mound at a rate of 4×10^{-7} cm/s. Gradients were almost linear in Hole 509, suggesting that a conductive thermal regime exists in the off-mounds area.

Manganese-oxide crusts have the highest density and sonic velocity, and the lowest porosity of all the sediments of this leg: wet-bulk density = 1.98 g/cm^3, grain density = 3.75 g/cm^3, porosity = 58.1%, sonic velocity = 2.22 km /s. The green clays have slightly higher density and sonic velocity and lower porosity than those of the previous sites: wet-bulk density = 1.66 g/cm^3, grain density = 3.12 g/cm^3, porosity = 70.1%, sonic velocity = 1.72 km/s. On the other hand, all of the physical properties of the pelagic sediments are similar to those of previous sites.

The preliminary results of the magnetic properties measurements on the sediments are very similar to those of Sites 506 and 507. However, the Mn-oxide crusts exhibit surprisingly coherent NRM directions despite their very low intensities, which are consistent with their presumably low Fe content.

In summary, the major differences between Site 509 sediments and those from the other sites are the following:

1) The manganese-crust fragments are much larger, and they form a thicker layer in Hole 509B. Moreover, the oxidized "mudline" layer is much thinner, and only ~0.7 meters of pelagic sediment overlay the hydro-

thermal material. These observations may indicate that Hole 509B was cored closer to the top of the mound than the other holes, and/or that the hydrothermal activity was more recent (or still active?) at this hole than at any other previous sites.

2) Contrary to sediment sections from other off-mounds holes, the lower halves of which are almost devoid of siliceous microfossils, Hole 509 contains such siliceous remains down to the bottom of the sedimentary column.

No basement drilling was attempted at this site.

REFERENCES

Drever, J. I., 1971. Magnesium-iron replacements in clay minerals in anoxic marine sediments. *Science*, 172:1334–1336.

Klitgord, K. D., and Mudie, J. D., 1974. The Galapagos Spreading Center: A near-bottom geophysical survey. *Geophys. J. R. Astron. Soc.*, 38:563–586.

Lonsdale, P., 1977. Deep-tow observations at the mounds abyssal hydrothermal field, Galapagos Rift. *Earth Planet. Sci. Lett.*, 36: 92–110.

McDuff, R. E., and Gieskes, J. M., 1976. Calcium and magnesium profiles in DSDP interstitial water: Diffusion or reaction? *Earth Planet. Sci. Lett.*, 53:1–10.

SITE 509 HOLE CORE (HPC) 1 CORED INTERVAL 0.0–1.0 m

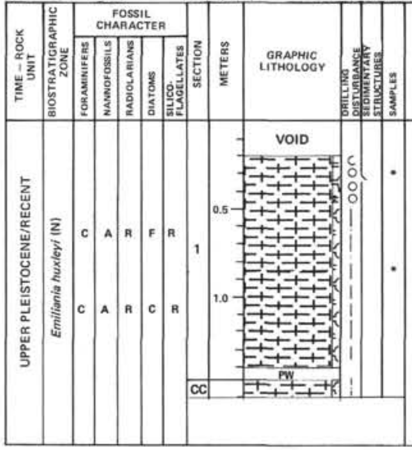

LITHOLOGIC DESCRIPTION

2.5Y 4/2

5GY 6/1

5GY 6/1
(5G 4/1)

5Y 5/3

5Y 6/1 to
5Y 4/1

SILICEOUS FORAMINIFER NANNOFOSSIL OOZE
Very dark grayish brown to greenish gray siliceous foraminifer nannofossil ooze. The top 20 cm of sediment recovered is the oxidized pelagic ooze which marks the mudline (sediment water interface). Mottling is present but it is hard to distinguish between drilling disturbance and biological activity.

SMEAR SLIDE SUMMARY (%)

	1-30	1-89
COMPOSITION:		
Clay minerals	2	TR
Micronodules	5	–
Carbonate unspec.	5	10
Foraminifers	5	10
Calc. nannofossils	70	60
Diatoms	10	10
Radiolarians	TR	5
Sponge spicules	TR	TR
Silicoflagellates	–	TR
Green clay	–	TR

SITE 509 HOLE CORE (HPC) 2 CORED INTERVAL 1.0–5.4 m

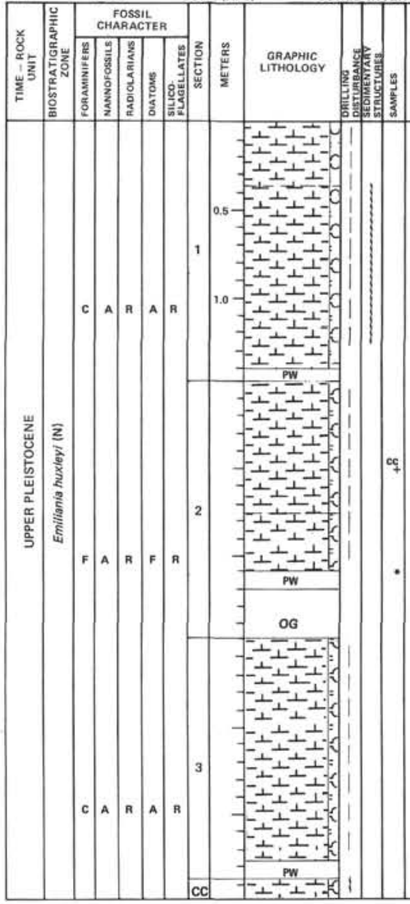

LITHOLOGIC DESCRIPTION

5Y 6/1

5G 6/1

5Y 5/2

5GY 6/1

5G 8/1
+
5G 6/1
+
N6

5Y 5/2

FORAMINIFER SILICEOUS NANNOFOSSIL OOZE
Burrowed, light olive gray to greenish gray foraminifer siliceous nannofossil ooze. Horizontal burrows of zoophycus(?) are scattered throughout Section 3. Some foraminifer are visible in the cores.

SMEAR SLIDE SUMMARY (%)

	2-109
COMPOSITION:	
Heavy minerals	TR
Clay minerals	TR
Volcanic glass (light)	TR
Zeolite	TR
Carbonate unspec.	5
Foraminifers	5
Calc. nannofossils	65
Diatoms	10
Radiolarians	5
Sponge spicules	TR
Silicoflagellates	TR
Green clay	TR

CARBON-CARBONATE (%)

	2, 43–45
Organic Carbon	2.46
Total Carbonate	49.0

SITE 509 HOLE CORE (HPC) 3 CORED INTERVAL 5.4–9.8 m

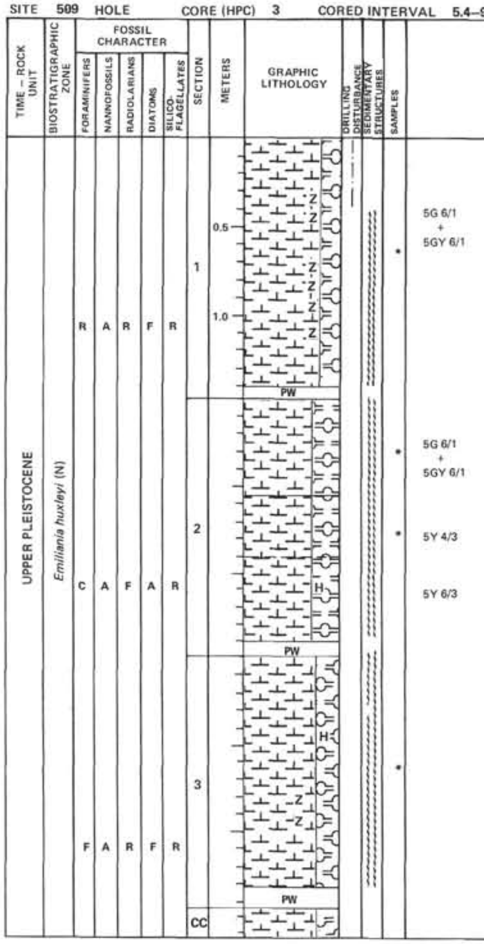

LITHOLOGIC DESCRIPTION

FORAMINIFER SILICEOUS NANNOFOSSIL OOZE and SILICEOUS FORAMINIFER NANNOFOSSIL OOZE

Variegated, multicolored, highly mottled, greenish gray pelagic ooze. Biogenic structures are well preserved. Zoophycus, planolites and halo burrows occur frequently. The dark gray vertical wisps and lines may be chrondrites? Large vertical burrows and branching burrows are observed. The pungent "rotten egg" odor associated with reducing conditions was detected.

SMEAR SLIDE SUMMARY (%)

	1-86	2-30	2-78	3-67
COMPOSITION:				
Clay minerals	5	5	3	3
Volcanic glass (light)	–	–	TR	TR
Carbonate unspec.	–	–	–	5
Foraminifers	5	15	10	5
Calc. nannofossils	60	30	55	60
Diatoms	10	25	20	20
Radiolarians	15	10	8	5
Sponge spicules	3	3	2	2
Silicoflagellates	TR	TR	TR	TR
Green clay	–	–	TR	–

SITE 509 HOLE CORE (HPC) 4 CORED INTERVAL 9.8–14.2 m

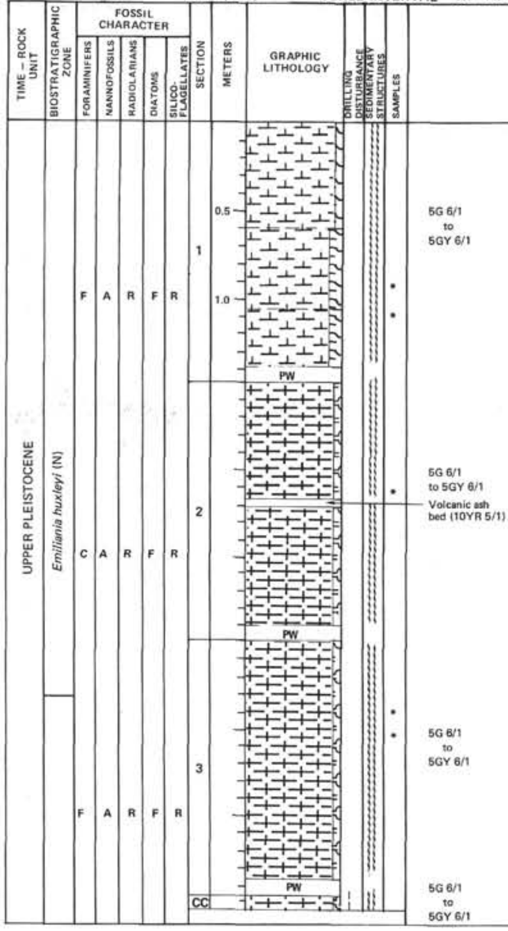

LITHOLOGIC DESCRIPTION

DIATOM NANNOFOSSIL OOZE to SILICEOUS FORAMINIFER NANNOFOSSIL OOZE

Greenish gray to grayish blue green, mottled pelagic ooze. Biogenic sedimentary structures are common, many displaying a variety of colors. Elongate, vertical, chondrites burrows are observed as well as the horizontal zoophycus burrows. Large burrows containing round opaques (pellets) are present.

VOLCANIC ASH LAYER

Section 2 at 64–67 cm contains a reddish gray volcanic ash layer. The volcanic glass is mostly acidic with basalt glass shards in minor abundance. It is distinct and contacts are well preserved.

SMEAR SLIDE SUMMARY (%)

	1-93	1-110	2-66 (ash)	2-78	3-40 (M)	3-55
COMPOSITION:						
Pyrite	–	TR	–	–	–	–
Amor. iron-oxide	–	TR	–	–	–	–
Other heavy minerals	–	–	5	–	–	–
Clay minerals	TR	2	–	5	–	3
Volcanic glass (light)	–	TR	75	–	–	–
Carbonate unspec.	5	–	–	–	–	2
Foraminifers	3	3	–	15	20	20
Calc. nannofossils	80	70	–	50	60	60
Diatoms	10	15	10	10	5	10
Radiolarians	2	3	10	15	5	3
Sponge spicules	1	2	TR	TR	–	1
Silicoflagellates	TR	1	–	TR	–	TR
Opaques	–	–	–	–	10	–

SITE 509 HOLE CORE (HPC) 5 CORED INTERVAL 14.2–18.6 m

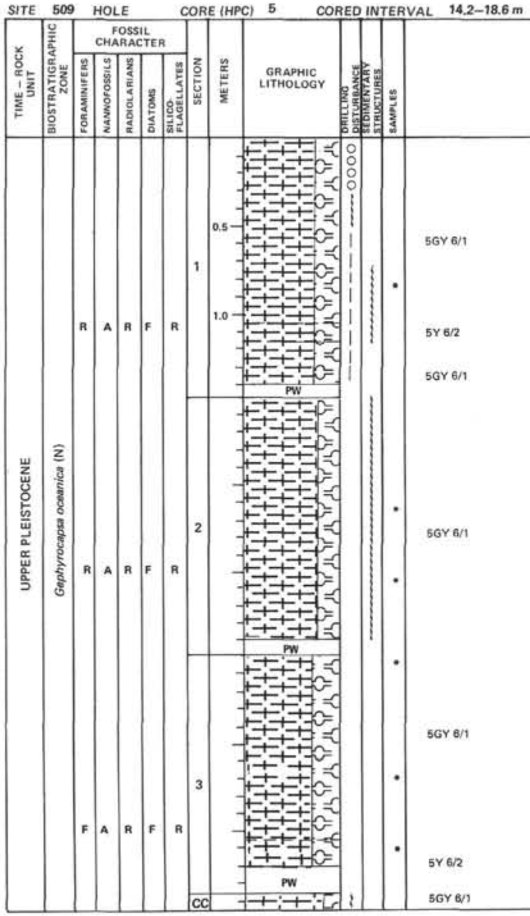

LITHOLOGIC DESCRIPTION

SILICEOUS FORAMINIFER NANNOFOSSIL OOZE

Mottled, greenish gray, light greenish gray, to pale olive, siliceous foraminifer nannofossil ooze. Foraminifer, radiolaria and diatoms occur in equal proportions. Trace fossils occur throughout the core with zoophycus burrows being the most common Void burrows with fecal pellets (opaques) occur. Major colors when they change over a few centimeters are considered gradational contacts.

SMEAR SLIDE SUMMARY (%)

	1-82	2-66	2-105	3-6	3-70	3-114
COMPOSITION:						
Pyrite	–	–	–	5	–	TR
Clay minerals	–	–	TR	TR	–	5
Volcanic glass (light)	TR	–	TR	–	TR	–
Carbonate unspec.	–	–	–	–	5	5
Foraminifer	15	15	2	–	10	3
Calc. nannofossils	50	50	75	70	50	65
Diatoms	15	15	15	15	15	15
Radiolarians	15	10	3	5	15	5
Sponge spicules	–	TR	–	2	–	2
Silicoflagellates	2	5	TR	–	3	TR
Opaques	3	5	–	5	–	–

SITE 509 HOLE CORE (HPC) 6 CORED INTERVAL 18.6–23.0 m

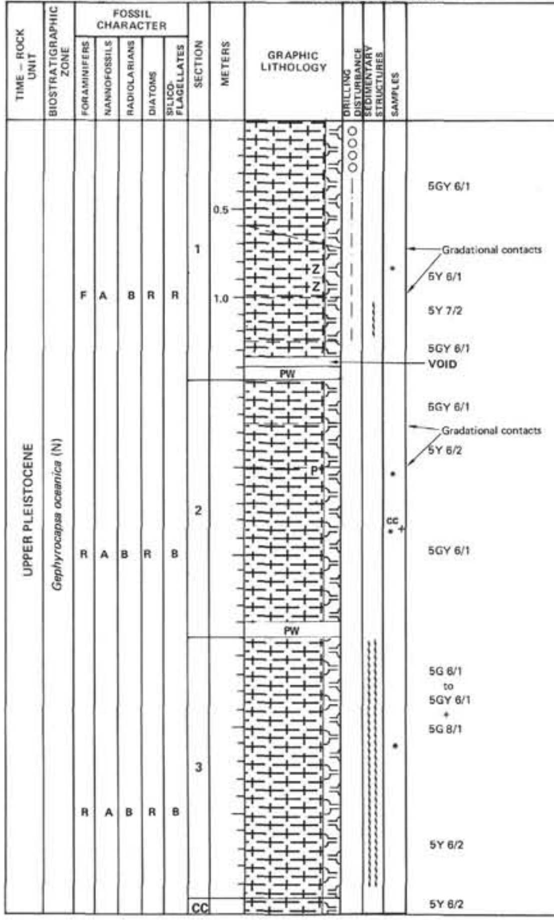

LITHOLOGIC DESCRIPTION

SILICEOUS FORAMINIFER NANNOFOSSIL OOZE

Variegated, light greenish gray to greenish gray siliceous foraminifer nannofossil ooze. The mottled character of the core is due to biogenic infauna. Planolites and zoophycus burrows are observed. Major changes in colors, if they occur over a few centimeters, are considered gradational contacts. Large void gray burrows are present. They are essentically the same composition but have a higher percentage of opaque nodules, which are most like fecal pellets.

SMEAR SLIDE SUMMARY (%)

	1-87	2-56 (M)	2-87	3-60
COMPOSITION:				
Clay minerals	TR	–	–	TR
Volcanic glass (light)	–	–	5	–
Carbonate unspec.	2	–	–	TR
Foraminifer	15	20	10	10
Calc. nannofossils	60	50	60	70
Diatoms	10	10	10	10
Radiolarians	10	10	10	10
Sponge spicules	3	TR	3	–
Opaques	–	10	–	–

CARBON-CARBONATE (%)

	2, 82–84
Organic Carbon	1.06
Total Carbonate	69.0

SITE 509 HOLE CORE (HPC) 7 CORED INTERVAL 23.0–27.4 m

TIME – ROCK UNIT	BIOSTRATIGRAPHIC ZONE	FOSSIL CHARACTER: FORAMINIFERS	NANNOFOSSILS	RADIOLARIANS	DIATOMS	SILICO-FLAGELLATES	SECTION
UPPER PLEISTOCENE	*Gephyrocapsa oceanica* (N)	F	A	B	F	B	1
		F	A	B	R	B	2
		C	A	R	F	B	3
							CC

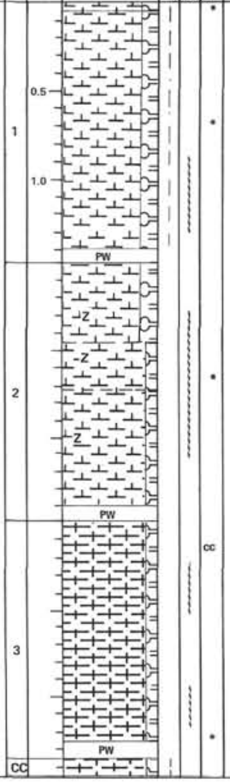

5Y 6/2
5GY 6/1
5GY 6/1
5Y 6/3
5GY 6/1
5GY 6/1
5GY 6/1

LITHOLOGIC DESCRIPTION

SILICEOUS NANNOFOSSIL OOZE to SILICEOUS FORAMINIFER NANNOFOSSIL OOZE

Multicolor, variegated, greenish gray to light greenish gray pelagic ooze. Biogenic sedimentary structure are common, zoophycus burrows being the most obvious.

SMEAR SLIDE SUMMARY (%)

COMPOSITION:	1-2	1-67	2-63	3-122
Pyrite	–	1	TR	–
Amor. iron-oxide	–	TR	–	–
Clay minerals	TR	TR	TR	TR
Volcanic glass (light)	–	–	–	TR
Carbonate unspec.	5	5	2	5
Foraminifers	5	5	3	15
Calc. nannofossils	67	80	80	65
Diatoms	15	13	10	10
Radiolarians	5	5	5	5
Sponge spicules	3	1	TR	TR
Silicoflagellates	–	TR	TR	TR

CARBON-CARBONATE (%)

	3, 10–12
Organic Carbon	1.28
Total Carbonate	81.0

SITE 509 HOLE CORE (HPC) 8 CORED INTERVAL 27.4–31.8 m

TIME – ROCK UNIT	BIOSTRATIGRAPHIC ZONE	FOSSIL CHARACTER: FORAMINIFERS	NANNOFOSSILS	RADIOLARIANS	DIATOMS	SILICO-FLAGELLATES	SECTION
UPPER PLEISTOCENE	*Gephyrocapsa oceanica* (N)	R	A	B	B	B	1
		C	A	B	B	B	2
		C	A	B	B	B	3
							CC

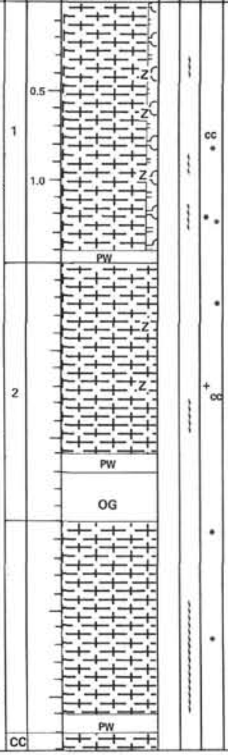

5GY 6/1
5GY 6/1
5GY 6/1
5GY 6/1

LITHOLOGIC DESCRIPTION

SILICEOUS FORAMINIFER NANNOFOSSIL OOZE to FORAMINIFER NANNOFOSSIL OOZE

Multicolored, mottled greenish gray to light greenish gray foraminifer nannofossil ooze. Biogenic sedimentary structures are common. Drilling disturbance is slight to non-existent. Zoophycus burrows are the most obvious.

SMEAR SLIDE SUMMARY (%)

COMPOSITION:	1-86	1-121 (M)	1-122	2-27	3-7	3-66
Pyrite	–	–	–	–	TR	–
Clay minerals	–	–	–	10	–	5
Volcanic glass (light)	–	–	–	2	TR	–
Carbonate unspec.	5	5	10	8	5	10
Foraminifers	15	15	10	15	15	3
Calc. nannofossils	60	70	70	65	75	80
Diatoms	5	2	3	TR	3	TR
Radiolarians	10	3	5	–	2	2
Sponge spicules	5	–	2	–	TR	TR

CARBON-CARBONATE (%)

	2, 78–81
Organic Carbon	0.82
Total Carbonate	67.0

SITE 509 HOLE CORE (HPC) 9 CORED INTERVAL 31.8–32.3 m

TIME – ROCK UNIT	BIOSTRATIGRAPHIC ZONE	FOSSIL CHARACTER: FORAMINIFERS	NANNOFOSSILS	RADIOLARIANS	DIATOMS	SILICO-FLAGELLATES	SECTION
							CC

5GY 6/1

LITHOLOGIC DESCRIPTION

FORAMINIFER NANNOFOSSIL OOZE

Greenish gray to light greenish gray foraminifer nannofossil ooze. The hydraulic piston corer hit basement, retrieving only the sediment caught in the Core-Catcher.

SITE 509 HOLE B CORE (HPC) 1 CORED INTERVAL 0.0–3.0 m

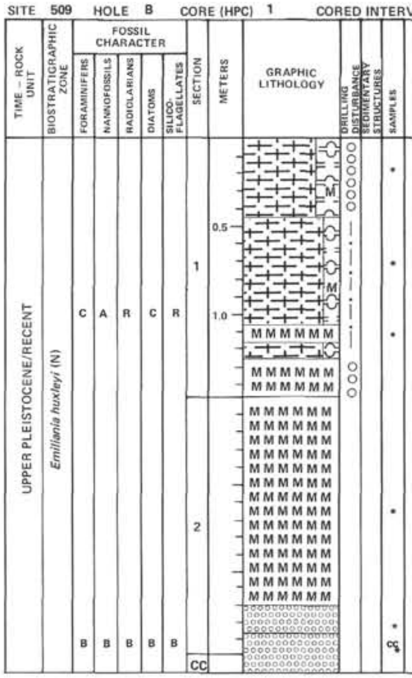

5YR 2/1

5YR 4/1
+
5Y 4/1

5YR 2/1
10YR 5/3
5YR 2/1

N1

10YR 4/6
2.5Y 3/2
2.5Y 3/2

LITHOLOGIC DESCRIPTION

PELAGIC OOZE mixed with and interbedded with HYDROTHERMAL SEDIMENTS

Highly disturbed, brownish black, brown, to olive gray siliceous foraminifer nannofossil ooze mixed with and interbedded with black Mn-oxide crust fragment. The sediments found at 0–45 cm is the oxidized pelagic ooze which marks the sediment-water interface. Fragments of Mn-oxide crust are mixed with pelagic ooze from 124 cm of Section 1. The rest of Section 1 and 120 cm of Section 2 is broken and fragmented Mn-oxide crust. Particles are flat pebbles to cobbles in size. The remainder of Section 2 is granular, dark grayish brown to dark yellowish brown hydrothermal clay. The granular clay is markedly distinct from the Mn-oxide crust.

SMEAR SLIDE SUMMARY (%)

	1-20	1-72	1-112	2-70	2-135	2-149
COMPOSITION:						
Amor. iron-oxide	–	5	–	20	–	–
Mn-crust	20	15	90	80	5	5
Foraminifers	5	10	5	TR	–	–
Calc. nannofossils	40	50	–	TR	–	–
Diatoms	20	10	5	TR	–	–
Radiolarians	10	10	–	TR	–	–
Sponge spicules	3	–	–	–	–	–
Silicoflagellates	2	–	–	TR	–	–
Green clay	–	–	–	–	95	95

SITE 509 HOLE B CORE (HPC) 2 CORED INTERVAL 3.0–7.4 m

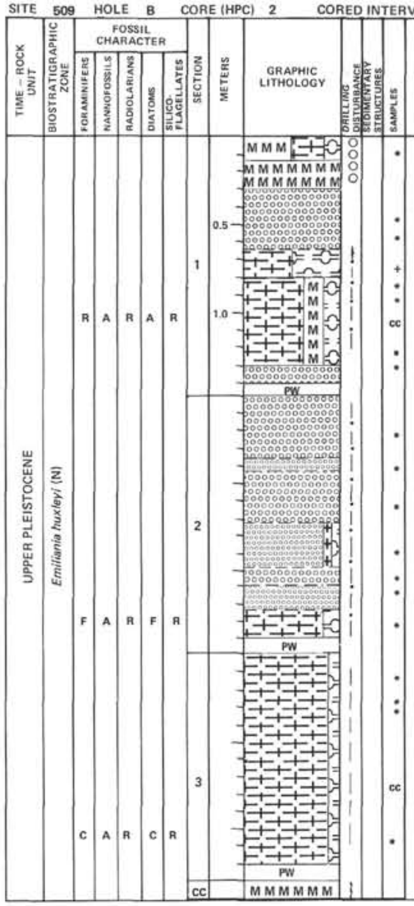

5Y 3/2
10YR 2/2

5Y 2.5/2

5Y 5/4

5Y 2.5/1–2

5Y 3/2

5Y 3/2
+
5G 4/1
5YR 4/1
5Y 3/2
+
5G 4/1

5G 4/1

5Y 3/2 +
5G 4/1
5G 4/1

5G 6/1

5G 8/1
to
5G 6/1

5YR 2/1

LITHOLOGIC DESCRIPTION

Mixed PELAGIC OOZE and HYDROTHERMAL SEDIMENTS

A dark olive brown, greenish gray to light greenish gray siliceous foraminifer nannofossil ooze mixed with and interbedded with black Mn-oxide crust fragments and dark olive brown granular clay. Mixing and contamination is present in the uppermost 30 cm. The zone from 60–125 cm in Section 1 may have been a series of alternating interbeds of ooze and Mn-oxide crust. Drilling disturbance has disrupted the sediments and only traces of bedding can be observed. Section 2 is dominantly a mixture of granular and fine grained cohesive green clay. This gradually mixes and grades into pelagic ooze which is found in Section 3.

SMEAR SLIDE SUMMARY (%)

	1-7	1-132	2-104	2-132	3-35	3-107
COMPOSITION:						
Clay minerals	–	–	–	5	–	TR
Volcanic glass (light)	TR	–	–	–	–	TR
Mn-crust	5	5	1	–	50	–
Zeolite	–	–	–	–	–	TR
Carbonate unspec.	5	–	–	5	–	10
Foraminifers	10	–	–	15	–	5
Calc. nannofossils	60	–	–	60	–	65
Diatoms	10	–	–	5	–	10
Radiolarians	7	–	–	15	–	5
Sponge spicules	2	–	–	2	–	–
Silicoflagellates	TR	–	–	TR	–	–
Green clay	–	95	99	–	50	–

CARBON-CARBONATE (%)

	3, 78–80
Organic Carbon	2.24
Total Carbonate	27.0

SITE 509 HOLE B CORE (HPC) 3 CORED INTERVAL 7.4–11.8 m

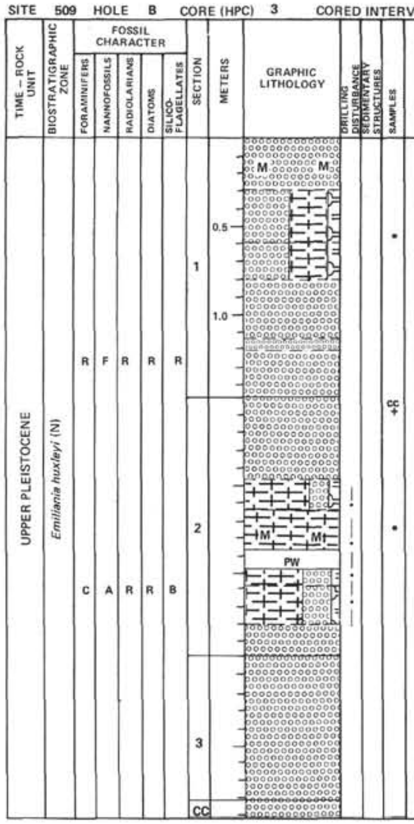

5GY 2/1
to
5G 2/1
+
5Y 2.5/1
5GY 2/1
to
5G 2/1
+
5Y 3/2
5Y 2.5/1
+
5Y 3/2
5GY 2/1
to
5G 2/1 +
5G 6/1
5GY 2/1
to
5G 2/1
N1
5GY 2/1
to
5G 4/1
10YR 8/3
+
5Y 8/1
5G 4/1 + 5Y 8/1 + 10YR 4/1
5G 4/1
to
5GY 2/1
N1
5GY 2/1
5GY 2/1

LITHOLOGIC DESCRIPTION

PELAGIC OOZE AND HYDROTHERMAL SEDIMENTS

Black Mn-oxide crust fragments, greenish black granular clay interlayered and mixed with siliceous foraminifer nannofossil ooze. Color variations are spectacular with textures of sediments changing from flat fragments to granules to cohesive less granular clay. The Mn-oxide crust is found only at the top of the core. It is mostly a contaminate which has fallen into the hole from higher up in the sediment column.

SMEAR SLIDE SUMMARY (%)

	1-57	2-75
COMPOSITION:		
Amor. iron-oxide	2	1
Clay minerals	TR	TR
Mn-crust	10	20
Carbonate unspec.	5	5
Foraminifer	10	15
Calc. nannofossils	55	50
Diatoms	10	TR
Radiolarians	5	5
Sponge spicules	TR	–
Silicoflagellates	–	TR

CARBON-CARBONATE (%)

	2, 6–8
Organic Carbon	0.13
Total Carbonate	2.0

SITE 509 HOLE B CORE (HPC) 4 CORED INTERVAL 11.8–16.2 m

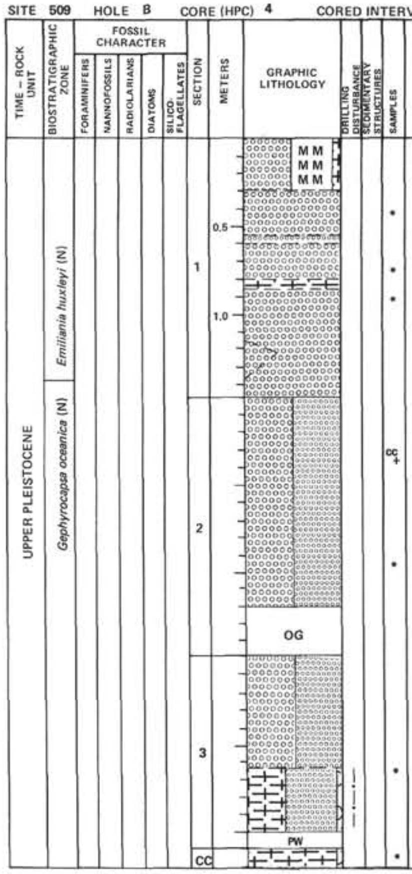

10YR 2/1
to
10YR 3/1
5GY 2/1
5G 6/1
5GY 2/1
5G 6/1
5GY 2/1
5G 6/1
5GY 2/1
to
N1
5GY 2/1
5GY 6/1 +
5G 4/1 +
5GY 2/1
5Y 4/2

LITHOLOGIC DESCRIPTION

HYDROTHERMAL SEDIMENTS

Greenish black to black granular clay mixed with and interbedded with a non-granular more cohesive dark greenish gray clay. Mn-oxide fragments are interpreted as being a contamination of sediment falling in the hole from up above. The contamination zone extends to 30 cm in Section 1. Siliceous foraminifer nannofossil ooze is mixed with granular and non-granular hydrothermal? clay in Section 3.

SMEAR SLIDE SUMMARY (%)

	1-40	1-69	1-95	2-98	3-68	CC-2
Volcanic glass (light)	–	–	–	TR	–	–
Mn-crust	5	–	–	–	–	–
Zeolite	–	10	–	1	TR	–
Micronodules	–	TR	–	–	–	–
Carbonate unspec.	TR	–	–	–	–	–
Calc. nannofossils	TR	–	–	–	–	–
Green clay	95	90	100	100	100	100

CARBON-CARBONATE (%)

	2, 34–36
Organic Carbon	0.10
Total Carbonate	1.0

SITE 509 HOLE B CORE (HPC) 5 CORED INTERVAL 16.2–20.6 m

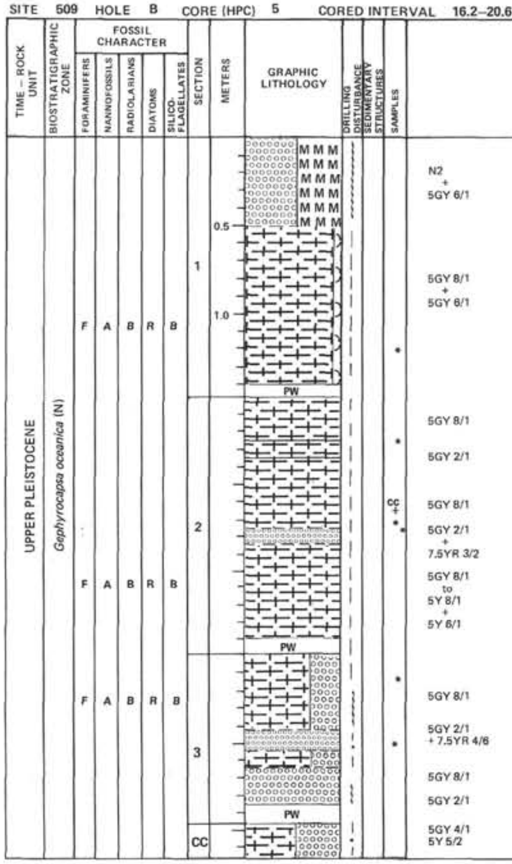

LITHOLOGIC DESCRIPTION

FORAMINIFER NANNOFOSSIL OOZE and HYDROTHERMAL SEDIMENT

Light greenish gray to greenish gray foraminifer nannofossil ooze mixed and interbedded with granular and non-granular greenish black to black clay. The pelagic ooze is dominant but contains many mottles or patches of green clay. Interbeds of granular and non-granular green clay with the pelagic ooze are found in the lower half of the core. The top 50 cm contains Mn-oxide fragments. This is interpreted as contamination from above.

SMEAR SLIDE SUMMARY (%)

	1-122	2-29	2-73	2-79	3-76	3-53
COMPOSITION:						
Amor. iron-oxide	–	–	–	50	–	–
Volcanic glass (light)	TR	–	–	–	–	–
Mn-crust	–	–	–	50	40	–
Zeolite	TR	–	–	–	–	–
Micronodules	TR	–	–	–	–	–
Carbonate unspec.	5	TR	5	–	–	–
Foraminifer	10	–	20	–	–	–
Calc. nannofossils	70	–	75	–	–	–
Diatoms	TR	–	–	–	–	–
Radiolarians	10	–	TR	–	–	–
Sponge spicules	TR	–	TR	–	–	–
Silicoflagellates	TR	–	–	–	–	–
Green clay	–	100	TR	TR	60	100

CARBON-CARBONATE (%)

	2, 61–63
Organic Carbon	1.65
Total Carbonate	78.0

SITE 509 HOLE B CORE (HPC) 6 CORED INTERVAL 20.6–25.0 m

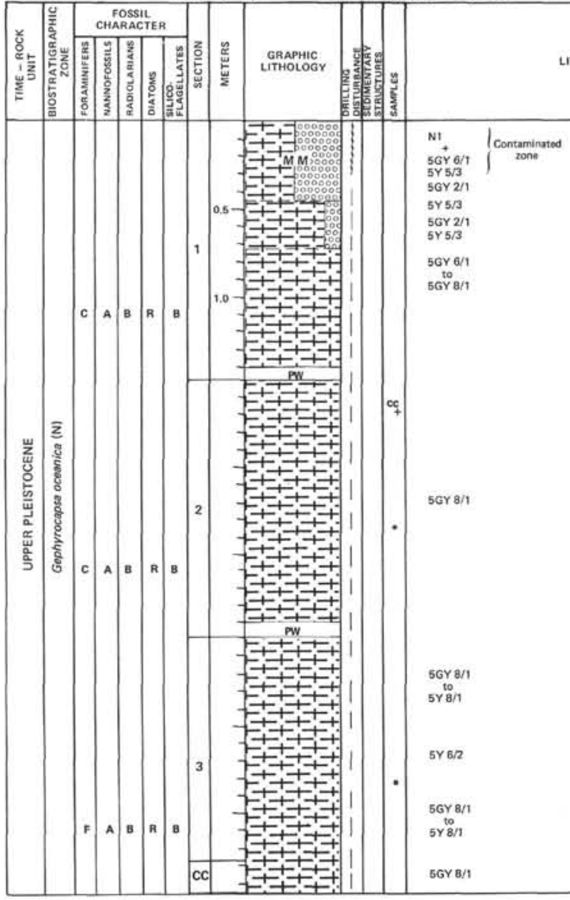

LITHOLOGIC DESCRIPTION

FORAMINIFER NANNOFOSSIL OOZE

Multicolor, dominantly greenish gray to light greenish gray foraminifer nannofossil ooze. Patches of green hydrothermal clay are scattered throughout the core. The upper 40 cm of the section consists of a mixture of black Mn-oxide fragments, greenish black granular hydrothermal clay and pelagic ooze. This is interpreted as a contamination zone and does not represent the true sediment lithology.

SMEAR SLIDE SUMMARY (%)

	2-85	3-83
COMPOSITION:		
Clay minerals	TR	TR
Volcanic glass (light)	TR	–
Zeolite	–	TR
Carbonate unspec.	10	10
Foraminifers	15	15
Calc. nannofossils	75	75

CARBON-CARBONATE (%)

	2, 11–13
Organic Carbon	1.14
Total Carbonate	70.0

SITE 509 HOLE B CORE (HPC) 7 CORED INTERVAL 25.0–29.4 m

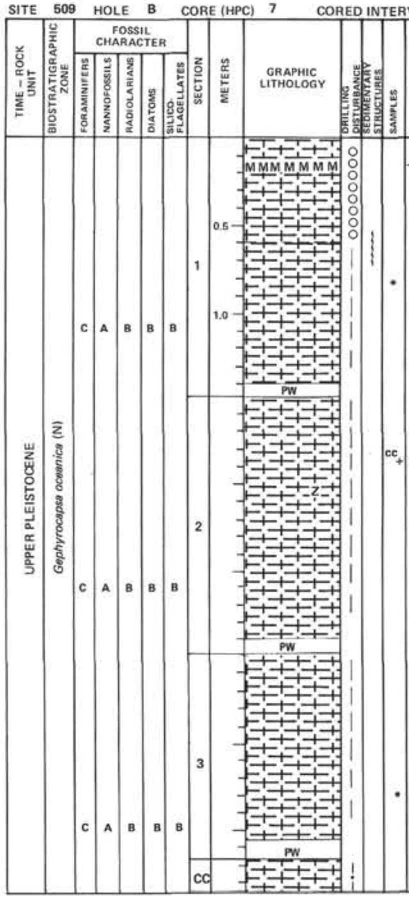

LITHOLOGIC DESCRIPTION

←Contamination

5G 8/1

5G 8/1

5GY 8/1

5GY 8/1

5GY 6/1

FORAMINIFER NANNOFOSSIL OOZE
Mottled and variegated, light greenish gray to greenish gray foraminifer nannofossil ooze. Zoophycus burrows are observed in Section 2. Patches of green hydrothermal clay are dispersed throughout the core.

SMEAR SLIDE SUMMARY (%)

	1-80	3-80
COMPOSITION:		
Clay minerals	–	TR
Micronodules	–	TR
Carbonate unspec.	10	10
Foraminifers	25	20
Calc. nannofossils	65	70
Diatoms	–	TR
Radiolarians	–	TR
Sponge spicules	–	TR

CARBON-CARBONATE (%)

	2, 33–35
Organic Carbon	1.12
Total Carbonate	84.0

SITE 509 HOLE B CORE (HPC) 8 CORED INTERVAL 29.4–32.8 m

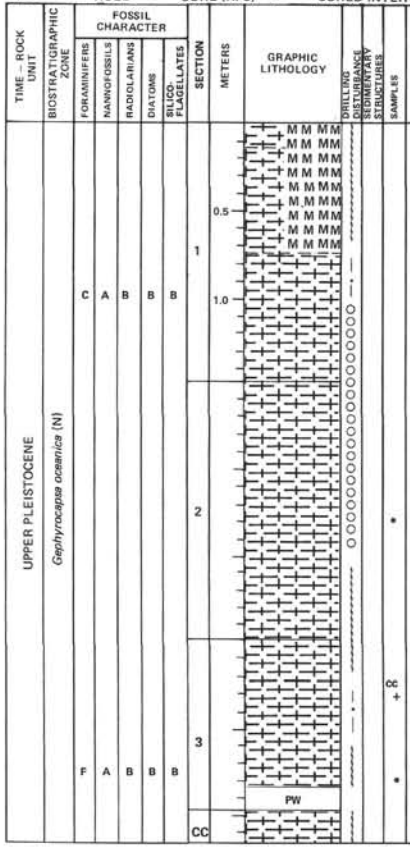

LITHOLOGIC DESCRIPTION

5GY 5/1
+ 7.5YR 3/2

Contaminated zone

5GY 8/1

5GY 8/1
to
5GY 6/1

5GY 8/1

5GY 8/1

5GY 8/1

FORAMINIFER NANNOFOSSIL OOZE
Light greenish gray to greenish gray foraminifer nannofossil ooze. This pelagic ooze is contaminated in the upper 77 cm with Mn-oxide fragments which have fallen into the core from up above. Drilling disturbance has obliterated any sedimentary structures which may have been present. Basaltic glass shards are observed in the lower section and in the Core-Catcher.

SMEAR SLIDE SUMMARY (%)

	2-80	3-80
COMPOSITION:		
Clay minerals	TR	TR
Volcanic glass (light)	TR	TR
Carbonate unspec.	10	10
Foraminifers	20	25
Calc. nannofossils	70	65

CARBON-CARBONATE (%)

	3, 28–30
Organic Carbon	0.84
Total Carbonate	71.0

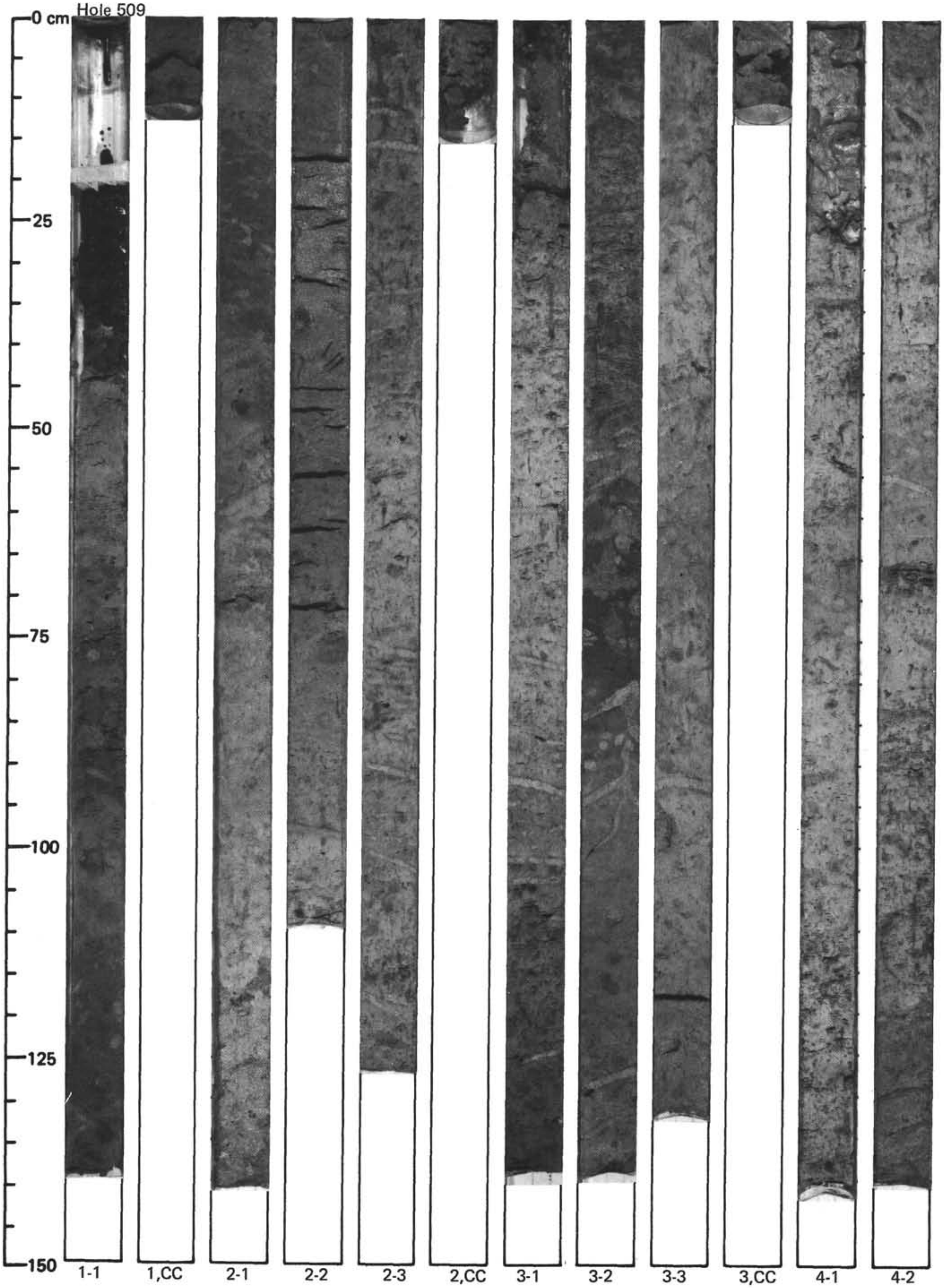
Hole 509
0 cm
25
50
75
100
125
150
1-1
1,CC
2-1
2-2
2-3
2,CC
3-1
3-2
3-3
3,CC
4-1
4-2

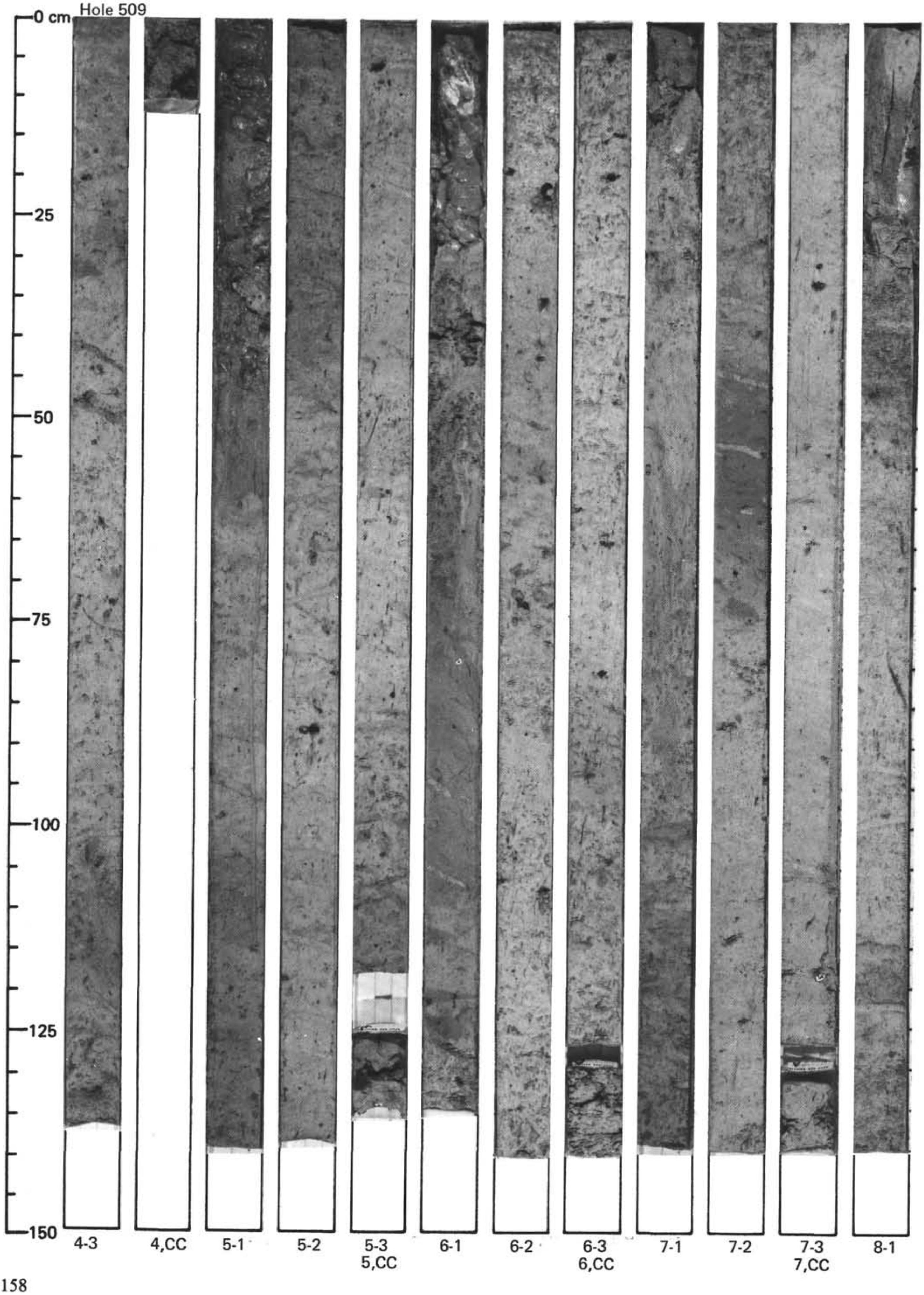
Hole 509
0 cm
25
50
75
100
125
150
4-3
4,CC
5-1
5-2
5-3
5,CC
6-1
6-2
6-3
6,CC
7-1
7-2
7-3
7,CC
8-1

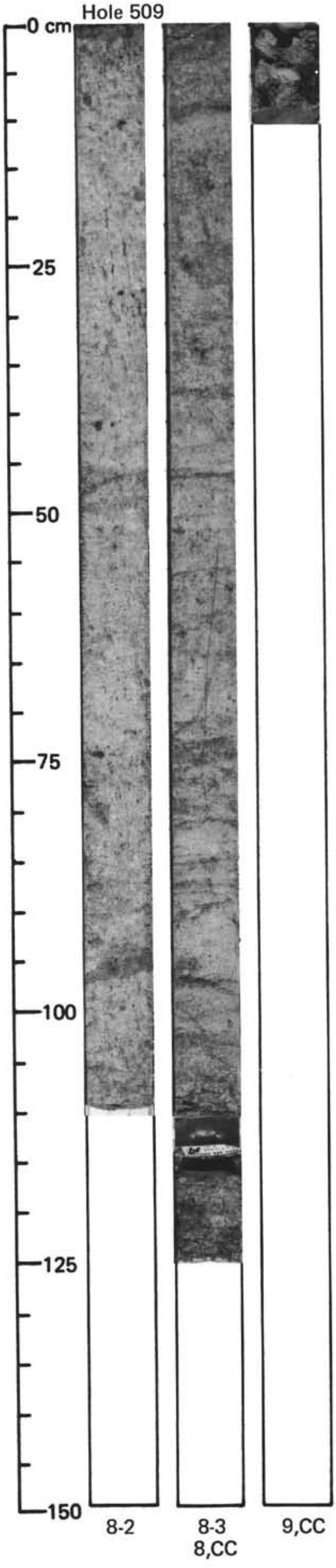
Hole 509
0 cm
25
50
75
100
125
150
8-2
8-3
8,CC
9,CC

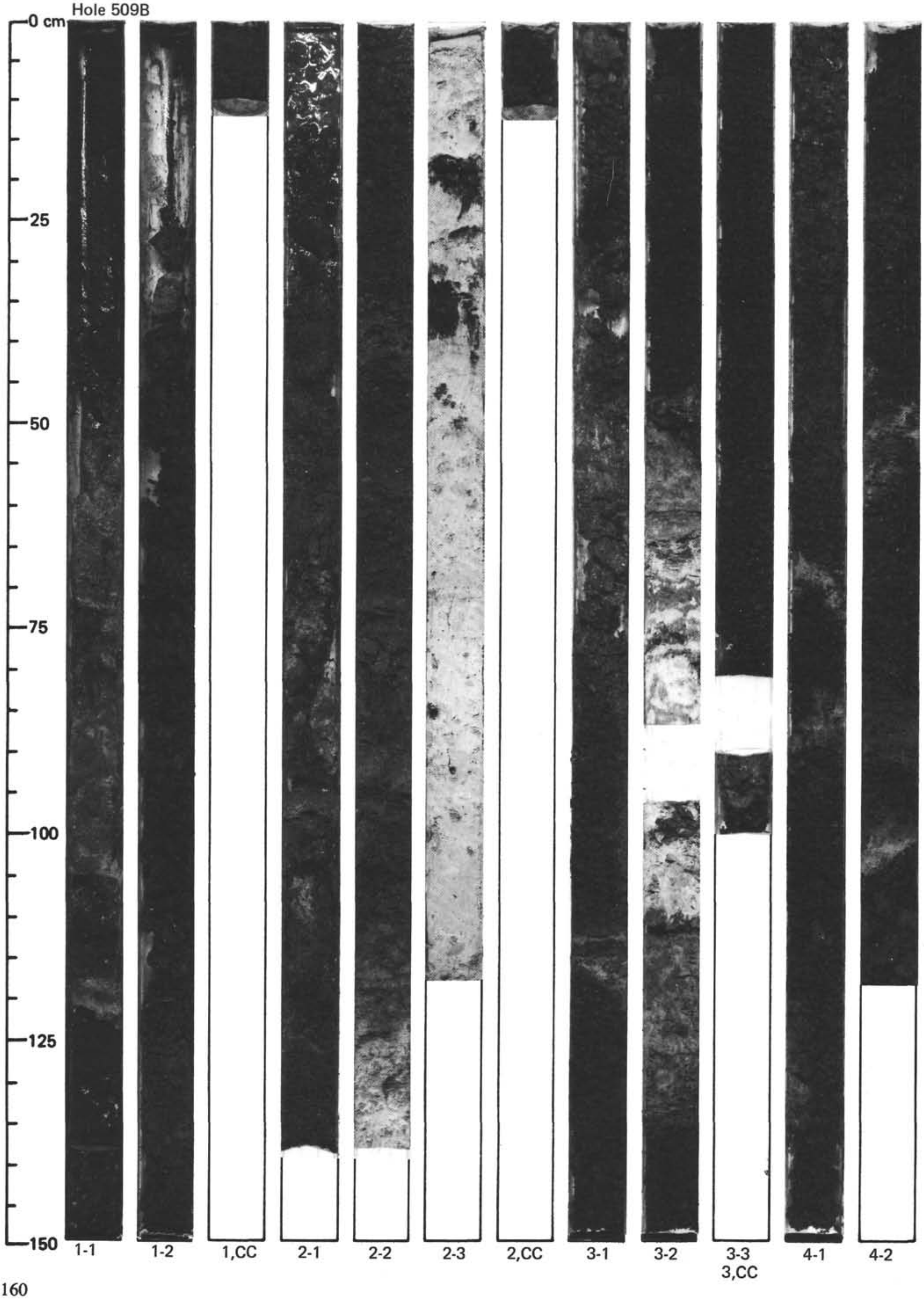
Hole 509B
0 cm
25
50
75
100
125
150
1-1
1-2
1,CC
2-1
2-2
2-3
2,CC
3-1
3-2
3-3
3,CC
4-1
4-2

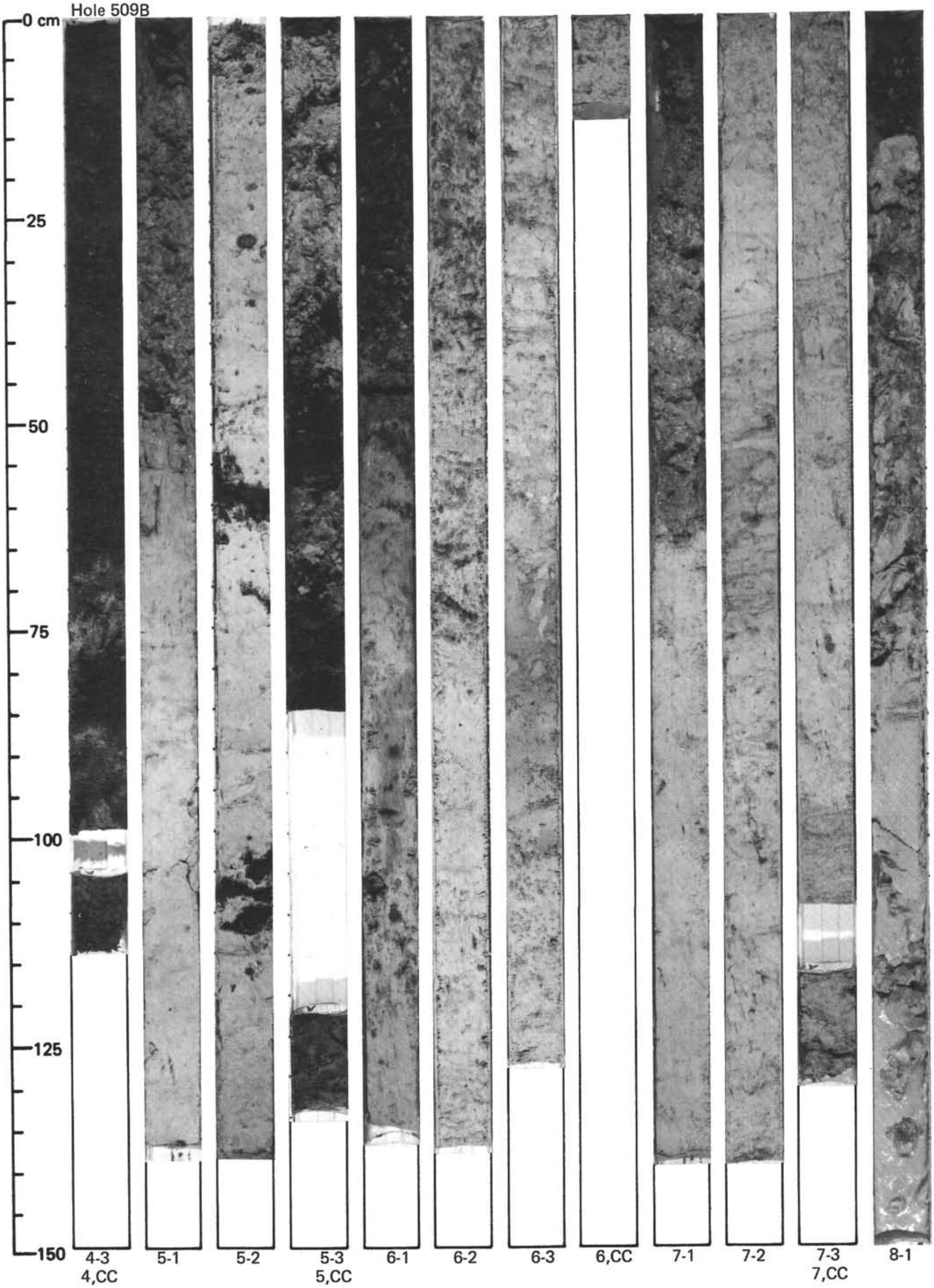
Hole 509B
0 cm
25
50
75
100
125
150
4-3
4,CC
5-1
5-2
5-3
5,CC
6-1
6-2
6-3
6,CC
7-1
7-2
7-3
7,CC
8-1

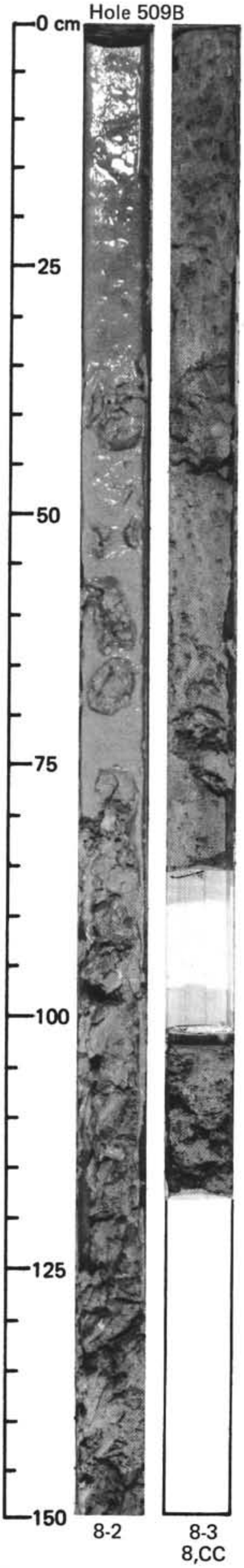
Hole 509B
0 cm
25
50
75
100
125
150
8-2
8-3
8,CC